NUREG/CR-6448
SSS-TR-95-15216
Vol. 1

Evaluation of National Seismograph Network Detection Capabilities

Annual Report
July 1994 – July 1995

Prepared by
K. L. McLaughlin, T. J. Bennett

S-CUBED Division of Maxwell Laboratories, Inc.

Prepared for
U.S. Nuclear Regulatory Commission

AVAILABILITY NOTICE

Availability of Reference Materials Cited in NRC Publications

Most documents cited in NRC publications will be available from one of the following sources:

1. The NRC Public Document Room, 2120 L Street, NW., Lower Level, Washington, DC 20555-0001

2. The Superintendent of Documents, U.S. Government Printing Office, P. O. Box 37082, Washington, DC 20402-9328

3. The National Technical Information Service, Springfield, VA 22161-0002

Although the listing that follows represents the majority of documents cited in NRC publications, it is not intended to be exhaustive.

Referenced documents available for inspection and copying for a fee from the NRC Public Document Room include NRC correspondence and internal NRC memoranda; NRC bulletins, circulars, information notices, inspection and investigation notices; licensee event reports; vendor reports and correspondence; Commission papers; and applicant and licensee documents and correspondence.

The following documents in the NUREG series are available for purchase from the Government Printing Office: formal NRC staff and contractor reports, NRC-sponsored conference proceedings, international agreement reports, grantee reports, and NRC booklets and brochures. Also available are regulatory guides, NRC regulations in the *Code of Federal Regulations*, and *Nuclear Regulatory Commission Issuances*.

Documents available from the National Technical Information Service include NUREG-series reports and technical reports prepared by other Federal agencies and reports prepared by the Atomic Energy Commission, forerunner agency to the Nuclear Regulatory Commission.

Documents available from public and special technical libraries include all open literature items, such as books, journal articles, and transactions. *Federal Register* notices, Federal and State legislation, and congressional reports can usually be obtained from these libraries.

Documents such as theses, dissertations, foreign reports and translations, and non-NRC conference proceedings are available for purchase from the organization sponsoring the publication cited.

Single copies of NRC draft reports are available free, to the extent of supply, upon written request to the Office of Administration, Distribution and Mail Services Section, U.S. Nuclear Regulatory Commission, Washington, DC 20555-0001.

Copies of industry codes and standards used in a substantive manner in the NRC regulatory process are maintained at the NRC Library, Two White Flint North, 11545 Rockville Pike, Rockville, MD 20852-2738, for use by the public. Codes and standards are usually copyrighted and may be purchased from the originating organization or, if they are American National Standards, from the American National Standards Institute, 1430 Broadway, New York, NY 10018-3308.

DISCLAIMER NOTICE

NUREG/CR–6448
SSS–TR–95–15216
Vol. 1

Evaluation of National Seismograph Network Detection Capabilities

Annual Report
July 1994 – July 1995

Manuscript Completed: November 1995
Date Published: March 1996

Prepared by
K. L. McLaughlin, T. J. Bennett

S–CUBED Division of Maxwell Laboratories, Inc.
La Jolla, CA 92038–1620

E. Zurflueh, NRC Project Manager

Prepared for
Division of Engineering Technology
Office of Nuclear Regulatory Research
U.S. Nuclear Regulatory Commission
Washington, DC 20555–0001
NRC Job Code L2170

Abstract

This first annual report presents detection thresholds, detection probabilities, and location error ellipse projections for the United States National Seismic Network (USNSN) with and without real-time cooperative stations in the eastern Unites States. Network simulation methods are used with spectral noise levels at stations in the USNSN and other stations to simulate the processes of excitation, propagation, detection, and processing of seismic phases.

The USNSN alone should be capable of detecting 4 or more P waves for shallow crustal earthquakes in nearly all of the eastern and central United States at the magnitude 3.8 level. When real-time cooperative stations are used in conjunction with the USNSN, the network should be capable of detecting 4 or more P waves from events 0.2 to 0.3 magnitude units lower. The planned expansion of the USNSN and cooperative stations should improve detection levels by an additional 0.2 to 0.3 magnitudes units in many areas. Location uncertainties for the USNSN should be significantly improved by addition of real-time cooperative stations. Median error ellipses for magnitude 4.5 earthquakes in the eastern and central US depend strongly upon location, but uncertainties should be less than 100 square km in the central United States and degrade to 200 square km or more off-shore and to the south and north of the international boundaries. Close cooperation with the Canadian National Network should substantially improve detection thresholds and location uncertainties along the Canadian border.

Table of Contents

List of Figures

List of Figures (Continued)

List of Figures (Continued)

List of Tables

1.0 Project Review

The research objective is to provide analysis that will allow evaluation of the quality and validity of seismic detections, event locations, magnitudes, focal mechanisms, moments, and corner frequencies for events throughout the eastern and central US based on data from the U.S. National Seismograph Network (USNSN). The project uses the Monte Carlo network simulation and analysis systems, XNICE and NetSim, to determine the capabilities of the USNSN to detect, locate, and characterize earthquake sources with or without the use of supplemental local seismic network data.

Results are expected to be useful for defining uncertainties in event locations, focal mechanisms, and other source parameters based on the USNSN and for determining criteria to identify what supplemental data could be used to improve uncertainties. Among the products of this research program will be maps covering the entire eastern and central U.S. which show detection thresholds, location uncertainty, and source characterization accuracy based on the evolving status of the USNSN alone and in combination with supplemental seismic stations. In addition, objective criteria will be developed for assessing earthquake source characterizations (e.g. focal mechanisms, moments, and corner frequencies) derived from the USNSN data as a function of location, depth, and magnitude/moment for the eastern and central U.S.

The first year's efforts have concentrated on predicting potential detection threshold and location uncertainties of the USNSN with and without cooperative seismic stations. Subsequent work will address the issues of source characterization (magnitude, focal mechanism, moments, and corner frequencies).

2.0 The USNSN and Cooperating Stations

Plans and specifications for the USNSN can be found in Buland (1993). The network consists of permanent 3-component observatory quality stations with direct real-time telemetry to the USGS NEIC. In addition, the network is augmented with direct real-time telemetry of quality stations provided by cooperating institutions. Operational and planned stations are listed in Tables 2.1a,b,c and their locations are shown in Figure 2.1. For reference, the seismic activity reported by the USGS for the region of the eastern US from Jan. 1994 to Sept. 1995 is shown in Figure 2.2.

Table 2.1a. Table of USNSN Stations - operating

Code	Lat.	Lon.	Station Name	Affiliation
AAM	42.300N	83.656W	Ann Arbor, MI	USGS
ALQ	34.943N	106.457W	Albuquerque, NM	USGS
BINY	42.199N	75.986W	Binghamton, NY	USGS
BLA	37.211N	80.421W	Blacksburg, VA	USGS
BMN	40.431N	117.222W	Battle Mtn., NV	USGS UNR
CBKS	38.814N	99.737W	Cedar Bluffs, KS	USGS SLU
CBM	46.932N	68.121W	Caribou, ME	USGS
CEH	35.891N	79.093W	Chapel Hill, NC	USGS
DUG	40.195N	112.813W	Dugway, UT	USGS ARPA
EYMN	47.946N	91.495W	Ely, MN	USGS AFTAC
GOGA	33.411N	83.467W	Godfrey, GA	USGS
GOL	39.700N	105.371W	Bergan Park, CO	USGS
GWDE	38.826N	75.617W	Greenwood, DE	USGS
JFWS	42.915N	90.249W	Mineral Point, WS	USGS SLU
LBNH	44.240N	71.926W	Lisbon, NH	USGS
LSCT	41.678N	73.224W	Lakeside, CT	USGS
MCWV	39.658N	79.846W	Mnt. Chateau, WV	USGS
MIAR	34.546N	93.573W	Mt. Ida, AR	USGS
MYNC	35.074N	84.128W	Murphy, NC	USGS
NEW	48.263N	117.120W	Newport, WA	USGS
OXF	34.512N	89.409W	Oxford, MS	USGS LLNL CERI
RSNY	44.548N	74.530W	Adirondack RS Obs., NY	USGS

RSSD	44.120N	104.036W	Black Hills RS Obs., SD	USGS
TPNV	36.929N	116.224W	Topapah, NV	USGS UNR
WMOK	34.738N	98.781W	Wichita Mtn., OK	USGS
WVOR	42.434N	118.637W	Wildhorse Valley, OR	USGS BR UNR
YSNY	42.476N	78.537W	Yorkshire, NY	USGS

Table 2.1b. Table of USNSN Stations - planned

Code	Lat.	Lon.	Station Name	Affiliation
COR	44.59N	123.30W	Corvalis, OR	Planned
DCTN	36.0N	88.0W	TN	Planned
MCSC	34.3N	81.3W	SC	Planned
OSOH	40.0N	83.1W	Columbus, OH	Planned
TUL	35.91N	95.79W	Leonard, OK	Planned
WCIN	39.1N	86.5W	IN	Planned
XXAL	31.1N	87.5W	AL	Planned
XXIL	40.5N	87.7W	IL	Planned
XXIO	41.0N	95.0W	IO	Planned
XXMN	44.0N	96.4W	MN	Planned
XXMO	36.6N	89.5W	New Madrid, MO	Planned
XXMS	34.9N	88.4W	MS	Planned
XXND	46.6N	100.3W	ND	Planned
XXRI	41.5N	71.3W	RI	Planned

Table 2.1c. Cooperating USNSN Stations (real-time)

Code	Lat.	Lon.	Station Name	Affiliation
CCM	38.056N	91.245W	Cathedral Cave, MO	IRIS
CMB	38.035N	120.383W	Columbia College, CA	BDSN
ELK	40.745N	115.239W	Elko, NV	LLNL
HRV	42.506N	71.558W	Harvard, MA	IRIS
HKT	29.950N	95.833W	Hockley, TX	IRIS USGS
ISA	35.663N	118.474W	Isabella, CA	TS
LTX	29.334N	103.667W	Lajitas, TX	AFTAC
MNV	38.433N	118.153W	Mina, NV	LLNL
PFO	33.609N	116.460W	Pinyon Flats Obs., CA	UCSD
SAO	36.765N	121.445W	San Andreas Obs., CA	BDSN
SSPA	40.636N	77.888W	Standing Stone, PA	IRIS
SMTC	32.949N	115.720W	Superstition Mtn., CA	TS

TUC	32.310N	110.784W	Tucson, AZ	IRIS
WDC	40.580N	122.540W	Whiskeytown Dam, CA	BDSN

Key to Affiliations and Participating Institutions:

AFTAC: Air Force Technical Applications Center, Patrick Air Force Base, Florida

ARPA: Advanced Research Projects Agency

BDSN: Berkeley Digital Seismograph Network, University of California-Berkeley, Berkeley, California

BR: Bureau of Reclamation

CERI: Center for Earthquake Research and Information, University of Memphis, Memphis, Tennessee

IRIS: Incorporated Research Institutions for Seismology

LLNL: Lawrence Livermore National Laboratory, Livermore, California

SLU: Saint Louis University, Saint Louis, Missouri

TS: Terrascope, California Institute of Technology, Pasadena, California

UCSD: University of California-San Diego

UNR: University of Nevada-Reno, Reno, Nevada

USGS: United States Geological Survey, Golden, Colorado

USNSN and Real-Time Cooperative Stations

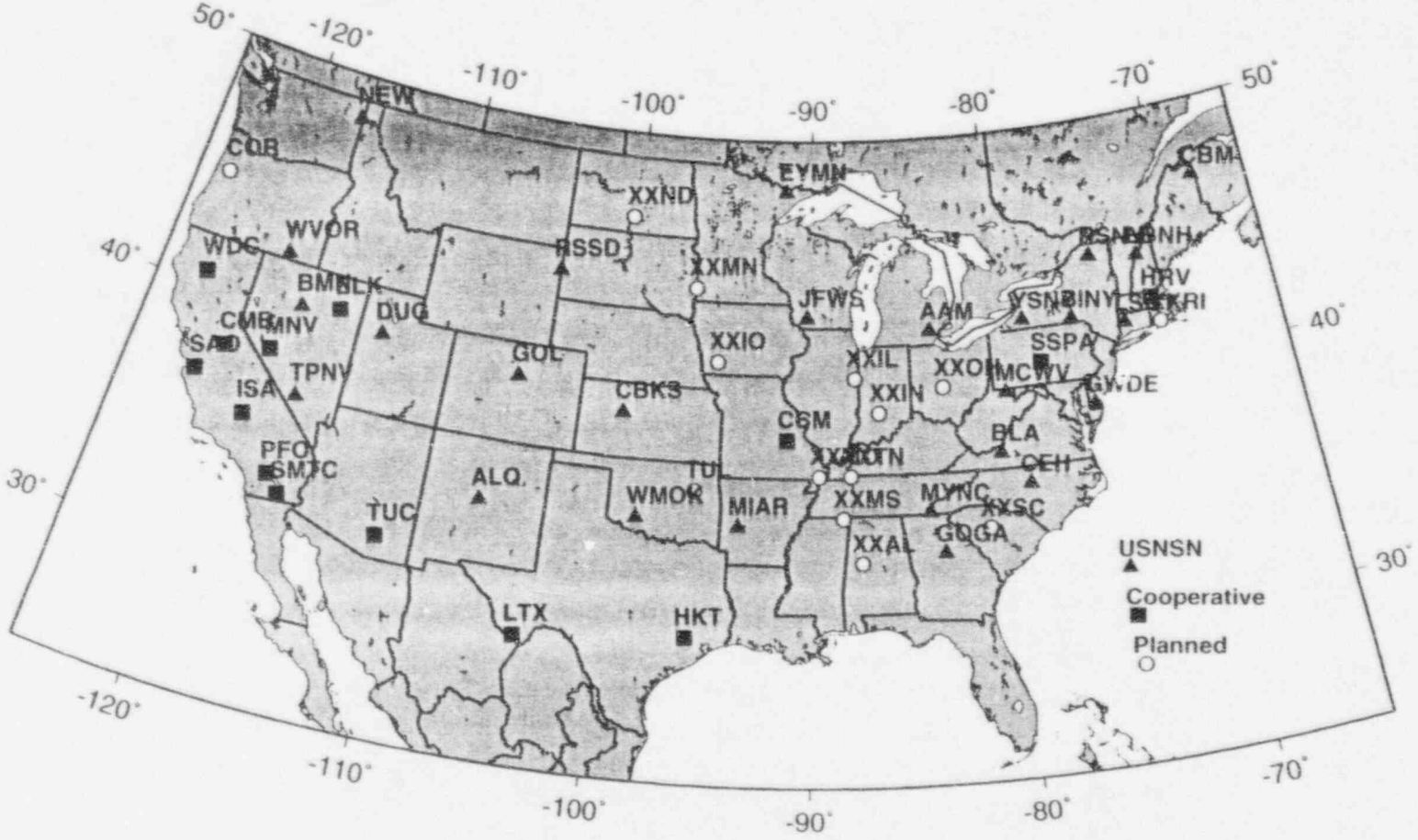

Figure 2.1 Map of USNSN and Cooperating Stations circa Sept. 1995.

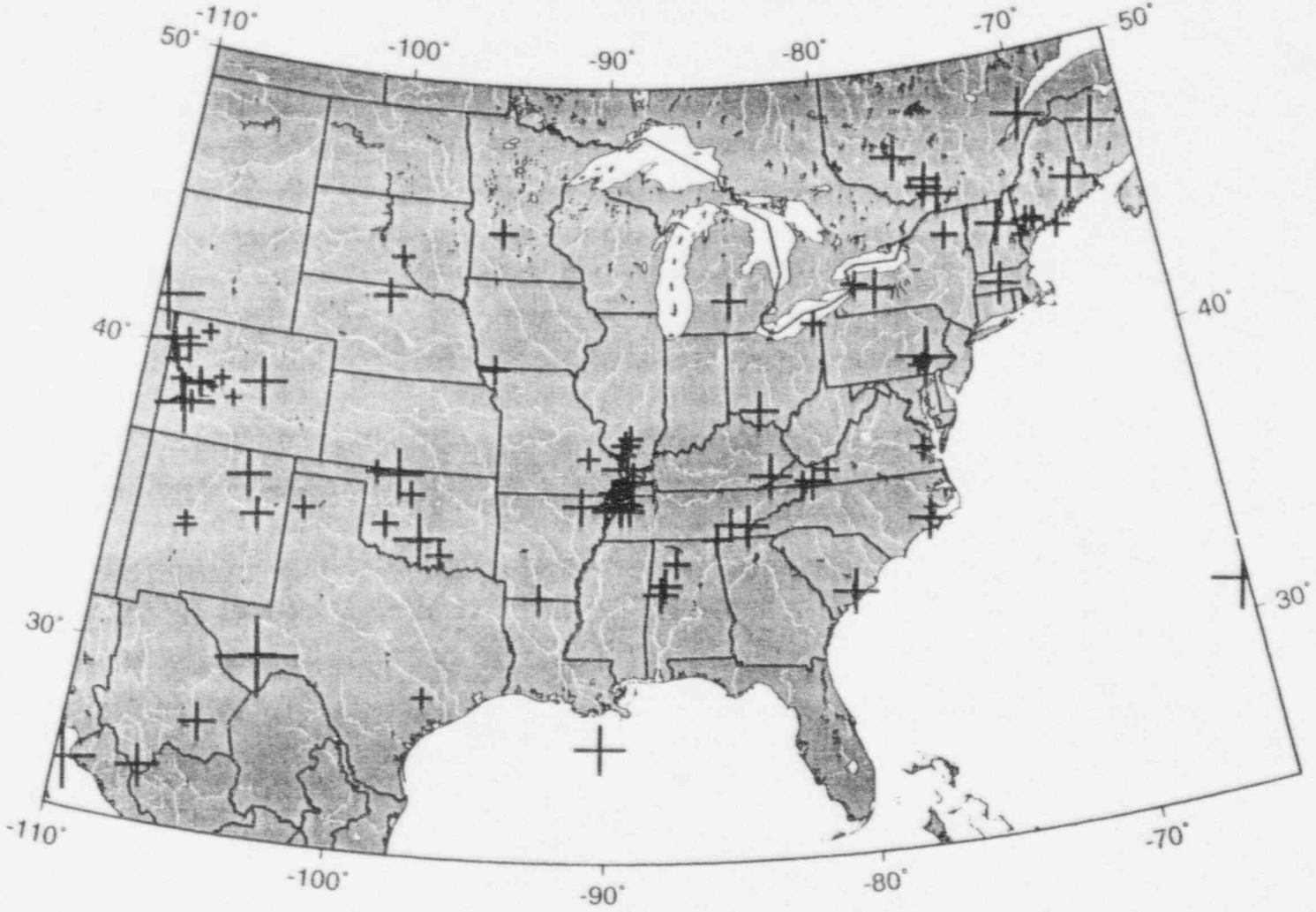

Figure 2.2 Map of seismicity reported in the region of the eastern US from Jan. 1994 to Sep. 1995 (from the USGS PDE Weeklies). Symbols size is proportional to magnitude; the smallest event on the map is magnitude 1.5, the largest is 5.7.

3.0 Introduction to Network Simulation and Capability Assessment

Network simulations are a way in which the capabilities of seismic networks can be predicted. It is common for these programs to be used in the planning and subsequent assessment of networks as they evolve with time. These capabilities include detection thresholds, location thresholds and uncertainties, and event characterization thresholds and uncertainties. The software and statistical basis for these network simulations is quite mature. Initial work was limited to the detection of 1 Hz teleseismic P-waves and limited analysis of location capabilities (Booker, 1964; and Wirth 1971) with the development of the NETWORTH and NETWORK programs. However, it was soon realized that these programs could be used to simulate detection and limited event characterization and identification capability using multiple seismic phases (Basham and Whitham, 1971). Subsequently the SNAP-D program was developed (Ciervo, *et al.*, 1985) which included short-period P- and S-waves as well as teleseismic short-period (1 Hz bandwidth) P- and S-waves, and long-period (20 second) Rayleigh waves. However, these programs could not fully analyze the highly nonlinear processes involved with broadband multi-phase location and event characterization. In order to fully analyze network identification capability it was found that the programs required more sophisticated Monte Carlo methods and multi-frequency simulation of many phase types to simulate regional networks and event characterization. To this end the two programs NICE (Barker, *et al.* 1986, 1994) and NetSim (Sereno, *et al.* 1990) were developed. NetSim built upon the traditional detection statistics of the SNAP-D program and added Monte Carlo event location capability while NICE embraced the Monte Carlo approach for both event detection determination as well as event location and identification modeling. Both NetSim and NICE use the same models for source, phase propagation, and detection. They differ in the approach to estimating simple detection thresholds but essentially use the same Monte Carlo approach for analysis of location capability. The NetSim program has not been extended to analyze the event characterization problem which is the purpose of the NICE program. Therefore we use the NetSim program for the estimation of simple detection capabilities and the NICE program for analysis of event characterization.

Network simulation methodologies use a model for the excitation and propagation of seismic phases from the source to the receiver and then use signal detection statistics to evaluate the probabilities of detection for a given source-receiver combination as a function of the event magnitude (or moment) and the noise levels at the station. Finally the procedures used in seismic bulletin generation are simulated to evaluate how well the available data will yield locations, magnitudes, and focal mechanisms for event characterization. Critical to this model is the partitioning of the process into four parts: source, path, receiver, and bulletin processing.

3.1 Source, S(f,M)

We need a description of the source strength as a function of frequency and magnitude or moment, S(f,M). For this purpose we scale a reference Brune source spectrum with moment, M. The low-frequency value of the source spectrum, S(f=0,M) = M, and the high-frequency asymptote is proportional to f^{-2}. We have used a nominal stress-drop set to 100 bars. A log-normal variation in source strength is assumed with a zero mean and a standard deviation, σ_S = 0.2 nominal.

3.2 Path, P(phase_type,f,).

Seismic logarithmic amplitudes must be specified as a function of phase type, distance, and frequency, P(phase_type,f). These attenuation functions are tabulated for the regional phases P, Pg, Pn, S, Sn, and Lg as well as the teleseismic phases, P, pP, sP, S, PKP, pPKP, sPKP, and LR. The propagation (attenuation) function is then assigned a standard deviation, σ_P = 0.2 nominal.

3.3 Receiver Effects, E(phase_type,station,f), and Noise, N(station,f).

Next we apply corrections for logarithmic station effects, E(phase_type,station,f). If the station is an array, then a frequency dependent array gain is applied for each phase type. In the case of the USNSN, we do not have any such corrections, but they are applied to teleseismic signals recorded on arrays such as at the Canadian, YKA array. If a station is found to have systematically smaller or larger amplitudes, then the correction may also be applied. Such corrections may be regressed for USNSN stations at a later date. The station corrections may also have standard deviations, $\sigma_E(f)$. Therefore, the predicted amplitude of a given phase is given by Log(A(phase_type,station,f,M)) = Log(S(f,M)) + P(phase_type,f) + E(phase_type,station,f)+ε, where ε is a random normal deviate with standard deviation, $\sigma_\varepsilon^2 = \sigma_S^2 + \sigma_P^2 + \sigma_E^2$.

A statistical model for the signal detection is next applied. The mean logarithmic noise levels as a function of frequency at each station are stored in tables, N(station,f), along with a standard deviation, $\sigma_N(f)$. The predicted logarithmic signal-to-noise ratio, SNR(phase_type,station,f,M) = Log(A) - N, has standard deviation, $\sigma_{SNR}^2 = \sigma_\varepsilon^2 + \sigma_N^2$. Since secondary regional phases such as S may be masked by coda from preceding arrivals such as Pg, a coda decay function is applied to the P phases. If the predicted coda level is above the ambient noise level then it is used instead of the ambient noise level.

We define the logarithmic signal-to-noise ratio of 0.5 as the 50% probability of detection and assume a cumulative normal for the probability of detection with standard deviation, σ_{SNR}. The total standard deviation is typically on the order of 0.5 to 0.7 depending upon the phase type and the station noise variability. A station reliability factor is applied, P_R(station), which is typically about 0.95 but may be reduced for less reliable stations. Also, we have found that we must discard low

probability detections (less than about 0.2 probability) in order to properly model network detections. Finally we write the probability of detection of a given phase at a specific station as a function of frequency and distance, and moment as

$$\Pr(\text{phase\_type, station, f, M,}\Delta) = P_R\ \Psi((\text{SNR}-0.5)/\sigma_{SNR}) \text{ if } P_R\ \Psi((\text{SNR}-0.5)/\sigma_{SNR}) \geq 0.2$$

and

$$\Pr(\text{phase\_type, station, f, M,}\Delta) = 0 \text{ if } P_R\ \Psi((\text{SNR}-0.5)/\sigma_{SNR}) < 0.2.$$

where $\Psi(x)$ is the normal cumulative probability function.

It is a straight forward exercise to directly compute the probability of m or more stations detecting a specified phase or combinations of phases using the above formula as a function of event location for a fixed moment or magnitude. The reader is directed to Ciervo, *et al.* (1985) for a discussion of the probability calculus involved. Similarly, it is possible to iterate on the probability calculation to determine at which magnitude (or moment) a specified probability of detection will be exceeded. These two types of calculations (magnitude threshold for fixed probability and probability for fixed magnitude) are the most common since they do not require Monte Carlo methods.

3.4 Bulletin Preparation

Once phases have been detected, the next step is the timing of arrivals, and the location of each event. We assume that all detected phases can be associated and we do not at this time attempt to model the phase association and event definition phase of analysis. Following event location, event characterization analysis such as focal mechanism determination or moment tensor inversion can proceed. The outcomes of these processes are strongly dependent upon the patterns of detections, signal-to-noise, and signal bandwidth. Monte Carlo methods have been developed to simulate these procedures. These Monte Carlo methods are used to simulate the statistics of the nonlinear estimation procedures by direct application of the procedures upon ensembles of synthetic data with detection patterns, random noise and travel time errors that are thought to capture the statistics of the errors in real data. At this time, our USNSN network simulations are limited to the simulation of event location only. Simulation of focal mechanism determination and centroid moment tensor (CMT) inversion are scheduled for years 2 and 3 of this project.

Location simulation proceeds as follows. For a fixed location and magnitude, up to 1000 events are randomly generated at the same location with detections at each station in the network. Arrival time errors are assigned to each detected phase, and a location algorithm is applied using P, Pn, Pg, S, Sn, Lg, and teleseismic P, S, and PKP. We have the option to assume that three component stations and/or arrays can estimate the arrival directions of P, Pn, Pg, teleseismic P and PKP with a specified standard deviation in direction. The errors in the location for each event in the ensemble are then tabulated and summary statistics are computed. These

summary statistics are tabulated on a grid of latitudes and longitudes and are contoured for display.

4.0 Noise Database

In order to conduct simulations we must have a noise model for each station. This noise model consists of the mean noise power as a function of frequency and a statistical variance for the noise level at each frequency. Of those stations in Table 2.1 we currently have noise models for stations: ALQ, BLA, DUG, LBNH, MIAR, MYNC, NEW, OXF, RSSD, RSNY, TUL, CCM, CMB, HRV, ISA, LTX, PFO, and TUC. For stations that we do not have noise models, we use surrogate stations in the same general region or a station located about the same distance to the coast. We expect to determine noise models for all stations in Table 2.1 in the second year of the project. Our current database contains noise models for about 500 historical and operating stations around the world (see Figure 4.1). Noise spectra for USNSN and real-time cooperative stations are shown in Figures 4.2a through 4.2r.

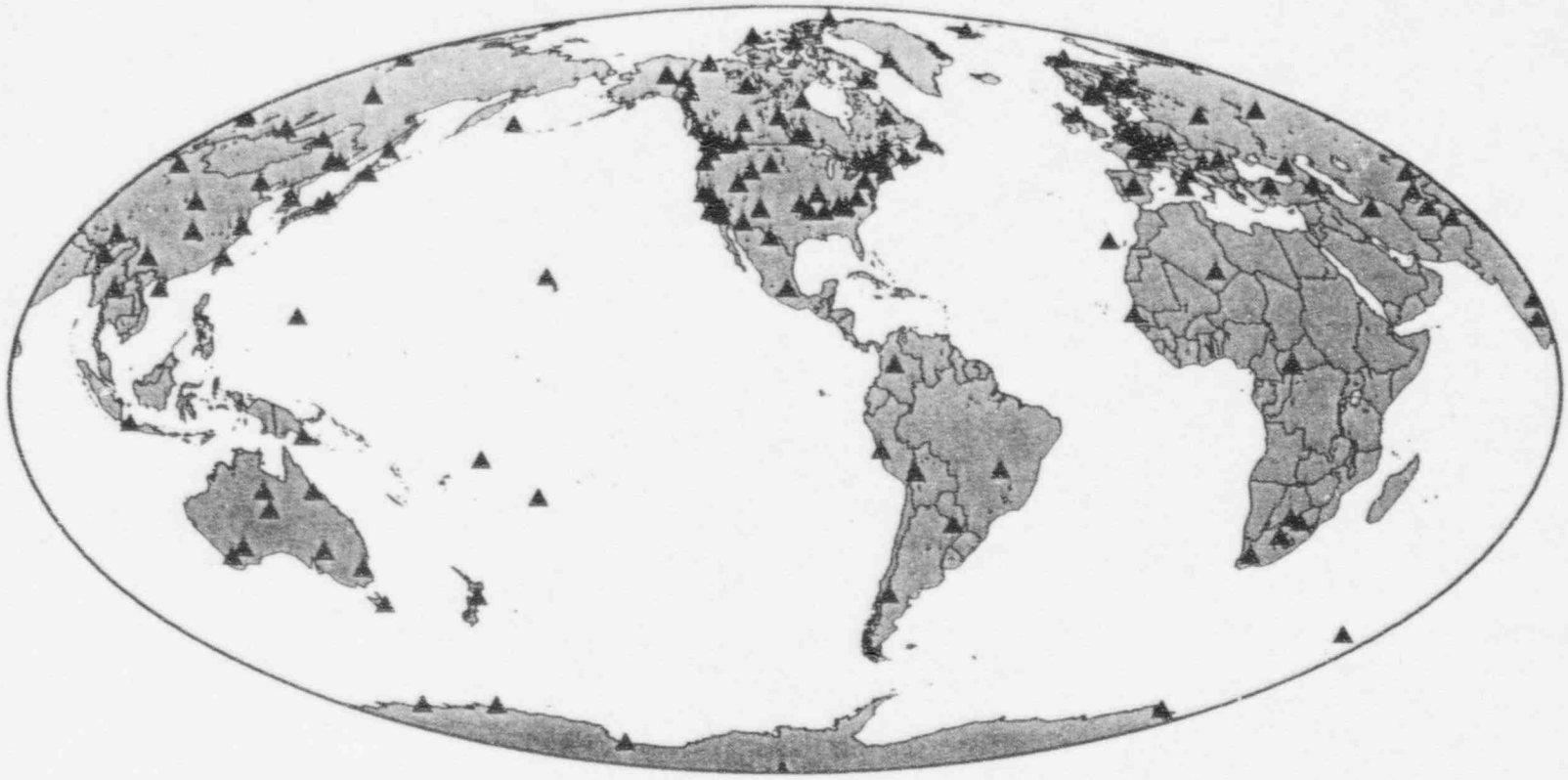

Figure 4.1 Map of world-wide noise database.

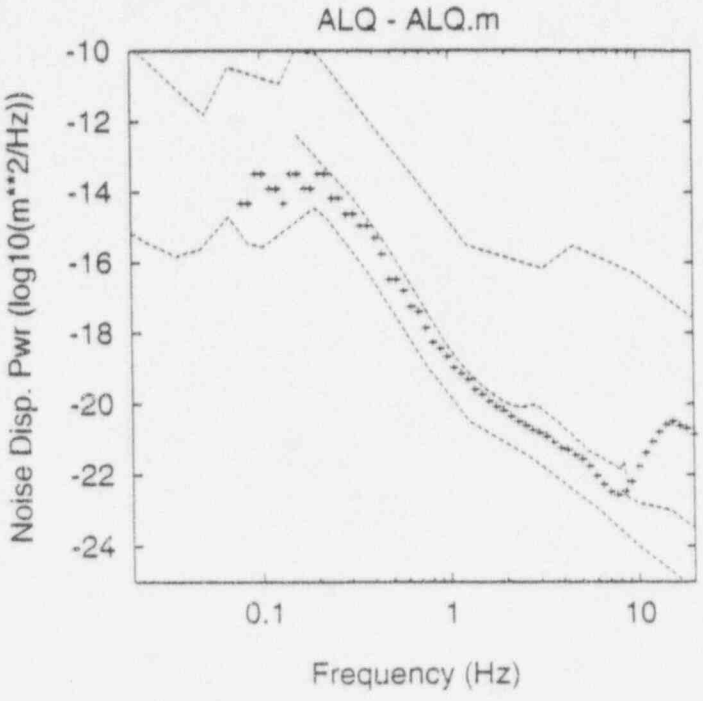

Figure 4.2a Spectral noise model for station ALQ. Crosses show the smooth mean noise level. Dotted lines show the USGS high noise model, the mean GTSN day time noise level, and the USGS low noise model. ALQ is a quieter than average station.

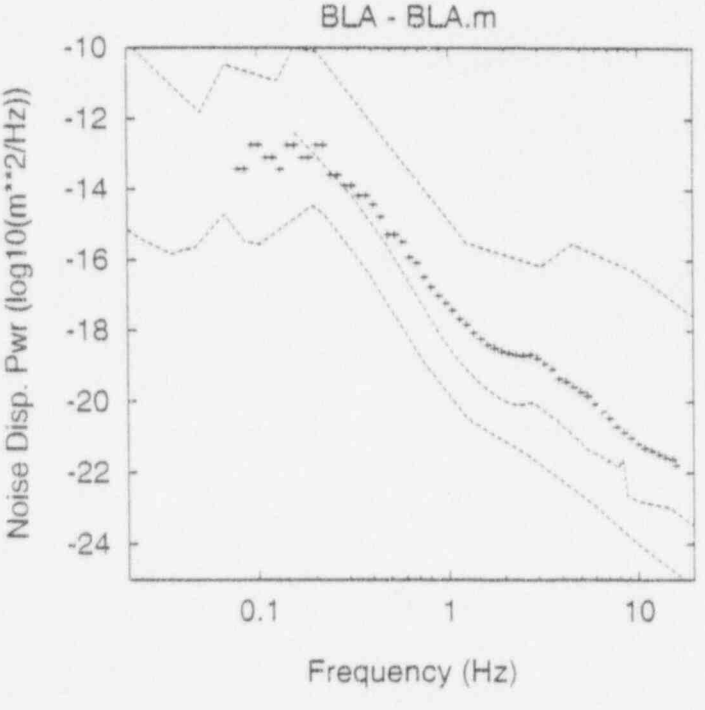

Figure 4.2b Spectral noise model for station BLA. Crosses show the smooth mean noise level. Dotted lines show the USGS high noise model, the mean GTSN day time noise level, and the USGS low noise model. BLA is a slightly noisier than average station.

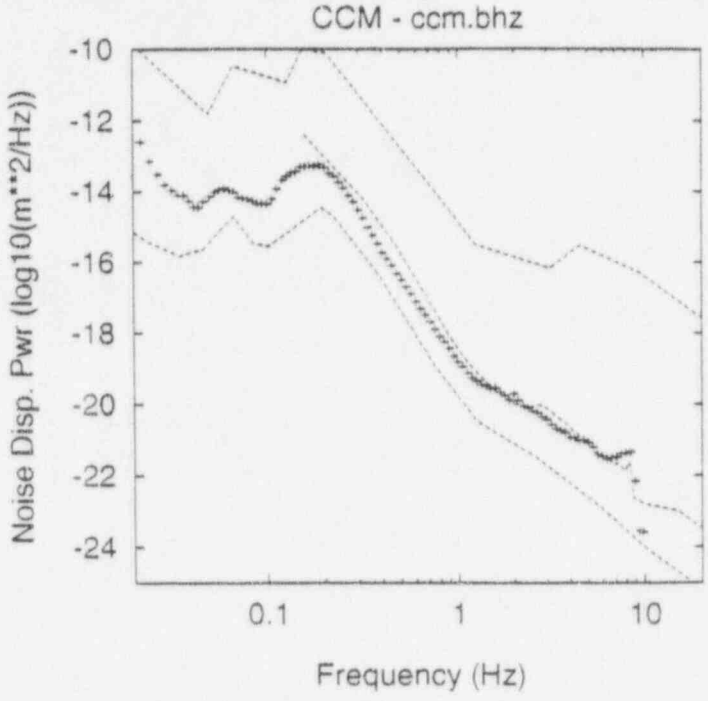

Figure 4.2c Spectral noise model for station CCM. Crosses show the smooth mean noise level. Dotted lines show the USGS high noise model, the mean GTSN day time noise level, and the USGS low noise model. CCM is a quieter than average station.

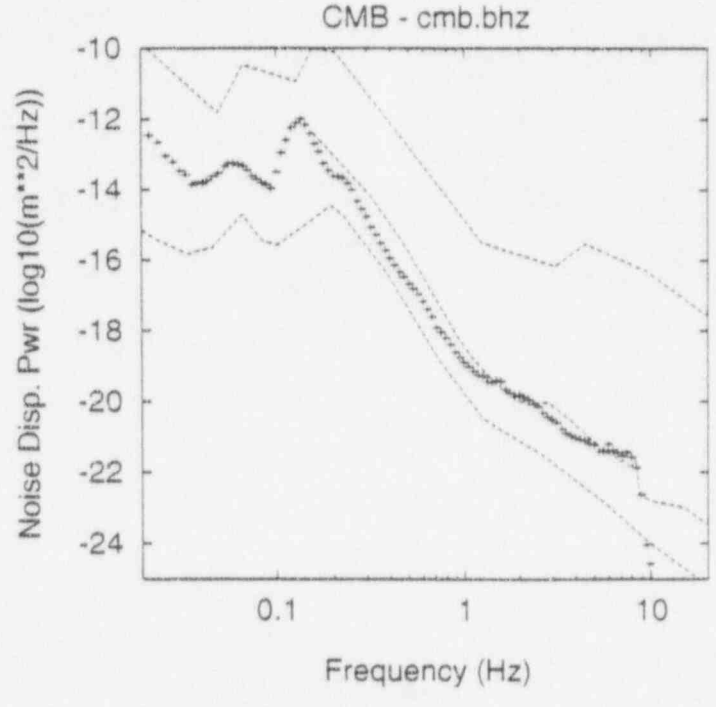

Figure 4.2d Spectral noise model for station CMB. Crosses show the smooth mean noise level. Dotted lines show the USGS high noise model, the mean GTSN day time noise level, and the USGS low noise model. CMB is a slightly quieter than average station.

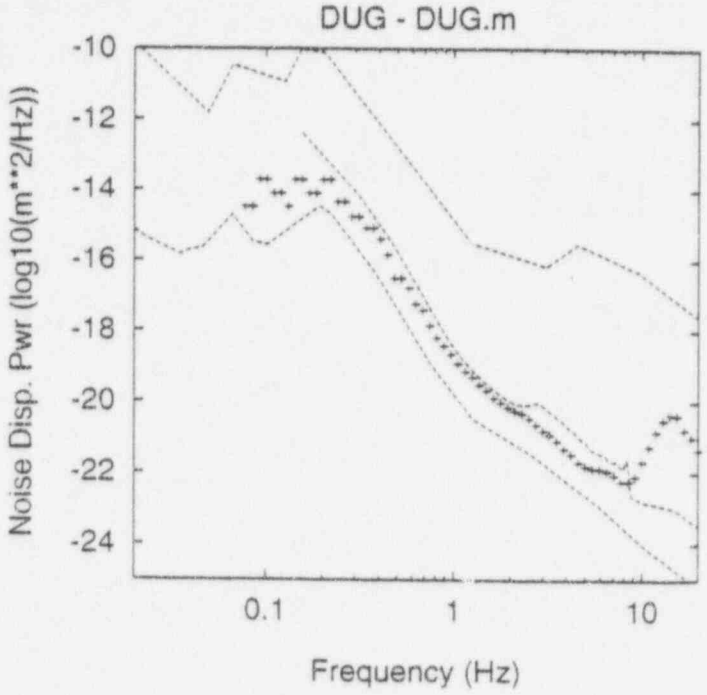

Figure 4.2e Spectral noise model for station DUG. Crosses show the smooth mean noise level. Dotted lines show the USGS high noise model, the mean GTSN day time noise level, and the USGS low noise model. DUG is a quieter than average station.

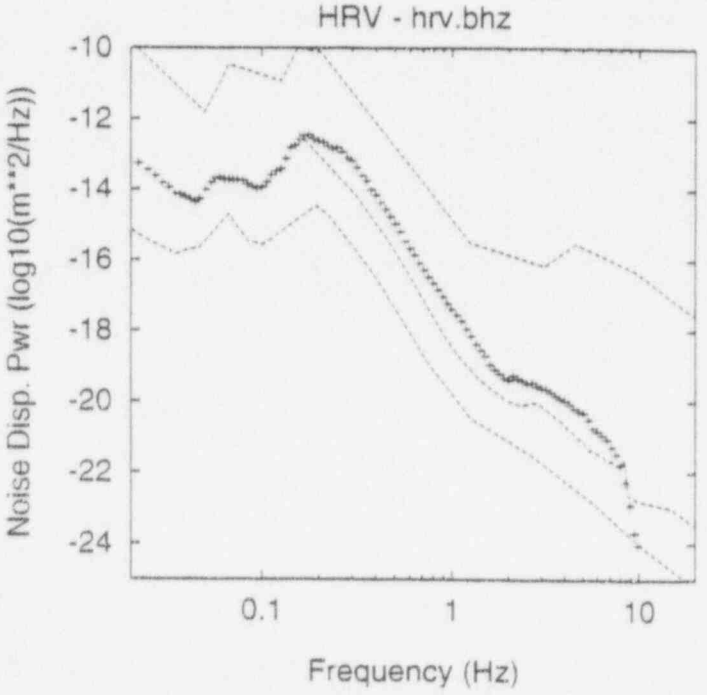

Figure 4.2f Spectral noise model for station HRV. Crosses show the smooth mean noise level. Dotted lines show the USGS high noise model, the mean GTSN day time noise level, and the USGS low noise model. HRV is a noisier than average station.

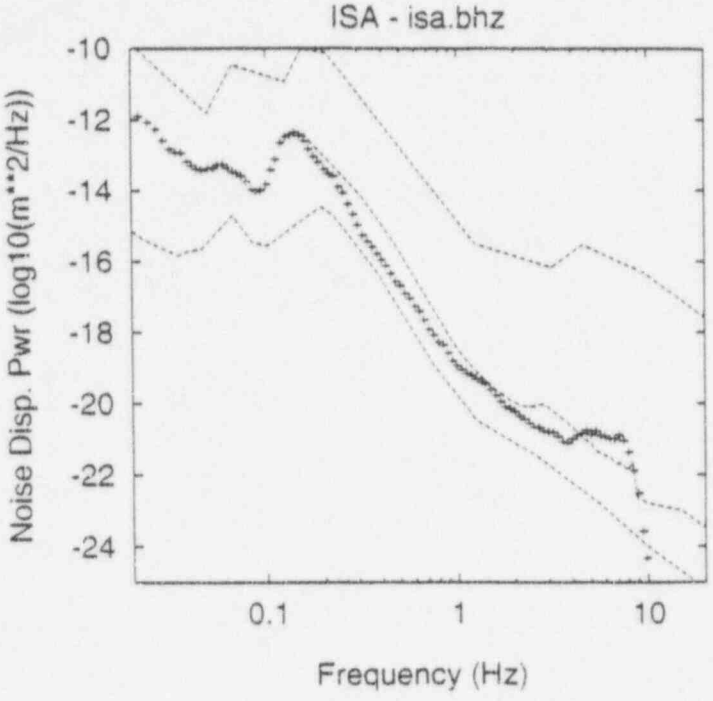

Figure 4.2g Spectral noise model for station ISA. Crosses show the smooth mean noise level. Dotted lines show the USGS high noise model, the mean GTSN day time noise level, and the USGS low noise model. ISA is a quieter than average station.

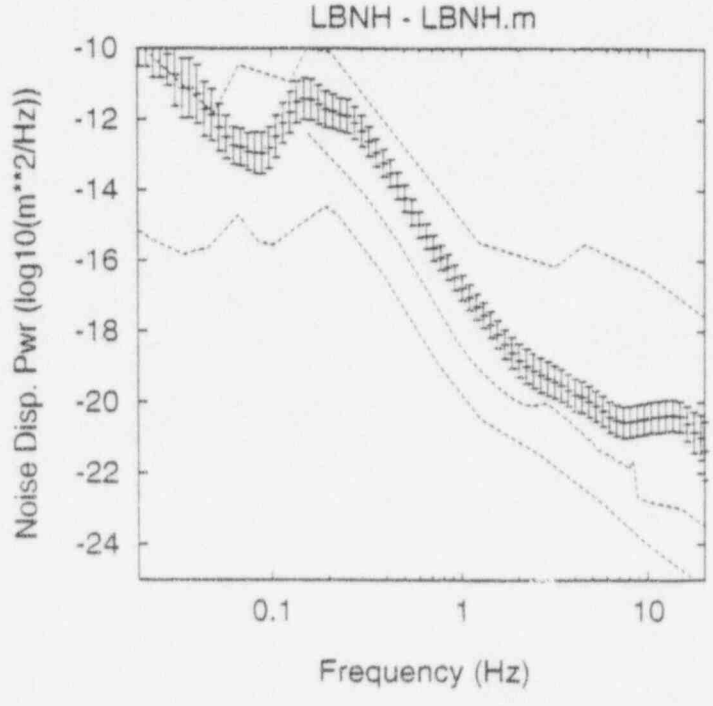

Figure 4.2h Spectral noise model for station LBNH. Crosses show the smooth mean noise level. Dotted lines show the USGS high noise model, the mean GTSN day time noise level, and the USGS low noise model. LBNH is a noisier than average station. Error bars show the variation in noise sampled.

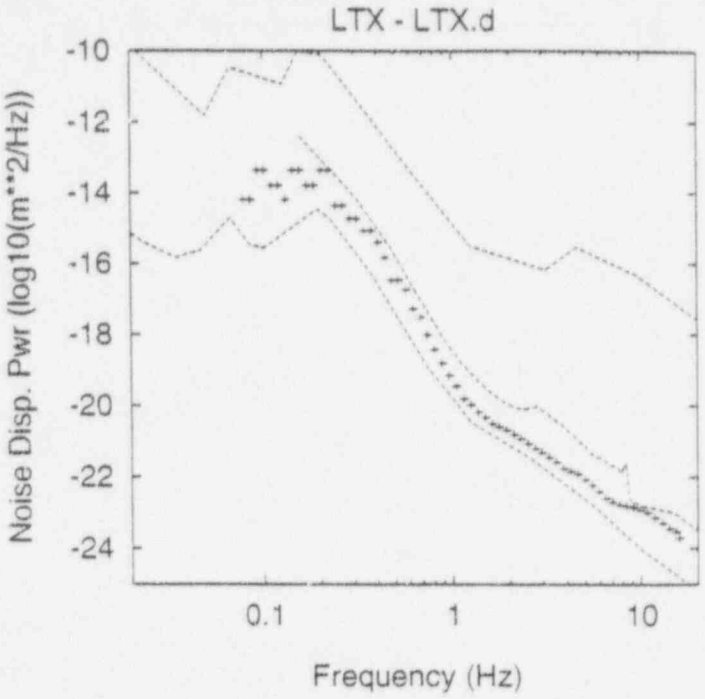

Figure 4.2i Spectral noise model for station LTX. Crosses show the smooth mean noise level. Dotted lines show the USGS high noise model, the mean GTSN day time noise level, and the USGS low noise model. LTX is a quieter than average station.

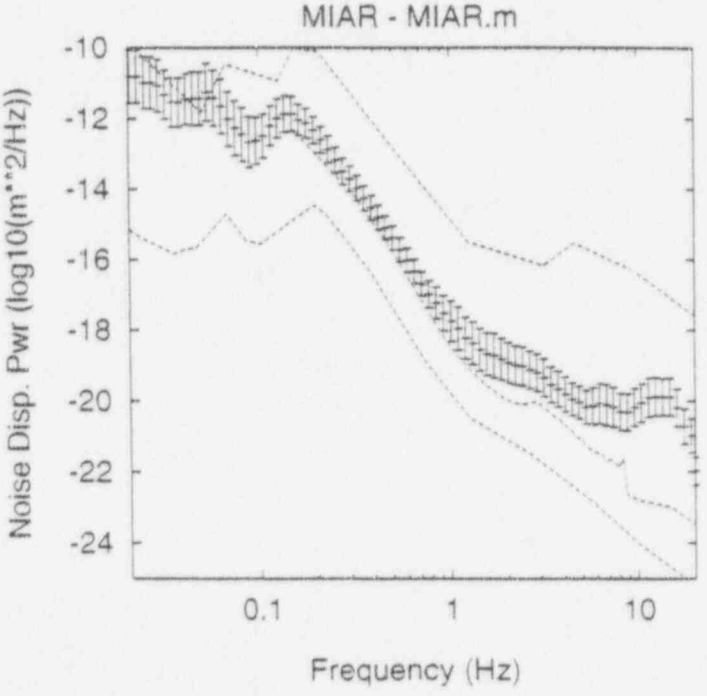

Figure 4.2j Spectral noise model for station MIAR. Crosses show the smooth mean noise level. Dotted lines show the USGS high noise model, the mean CTSN day time noise level, and the USGS low noise model. MIAR is a noisier than average station. Error bars show the variation in noise sampled.

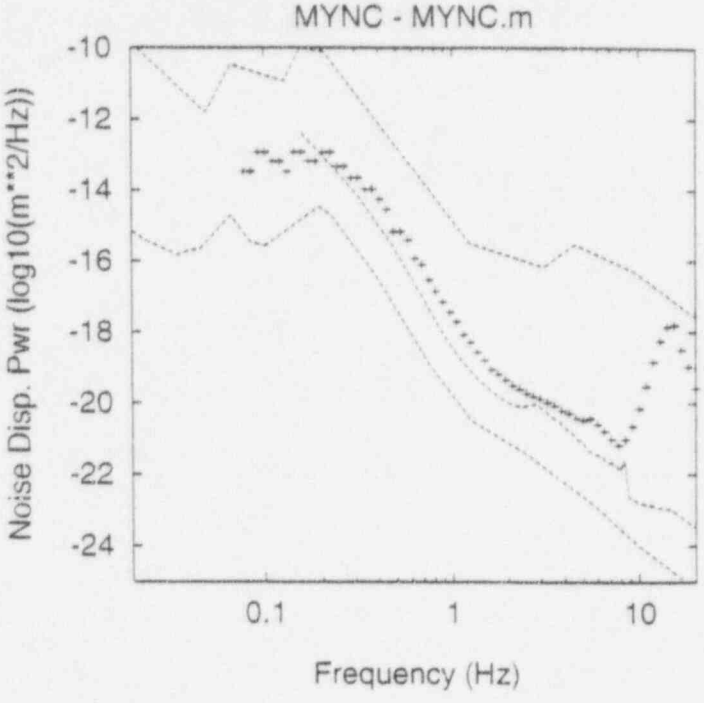

Figure 4.2k Spectral noise model for station MYNC. Crosses show the smooth mean noise level. Dotted lines show the USGS high noise model, the mean GTSN day time noise level, and the USGS low noise model. MYNC is a noisier than average station.

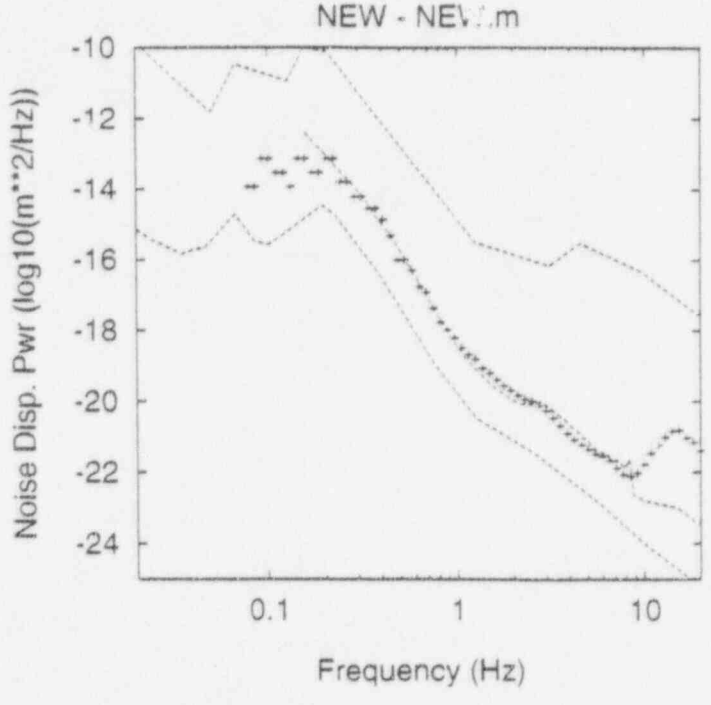

Figure 4.2l Spectral noise model for station NEW. Crosses show the smooth mean noise level. Dotted lines show the USGS high noise model, the mean GTSN day time noise level, and the USGS low noise model. NEW is an average station.

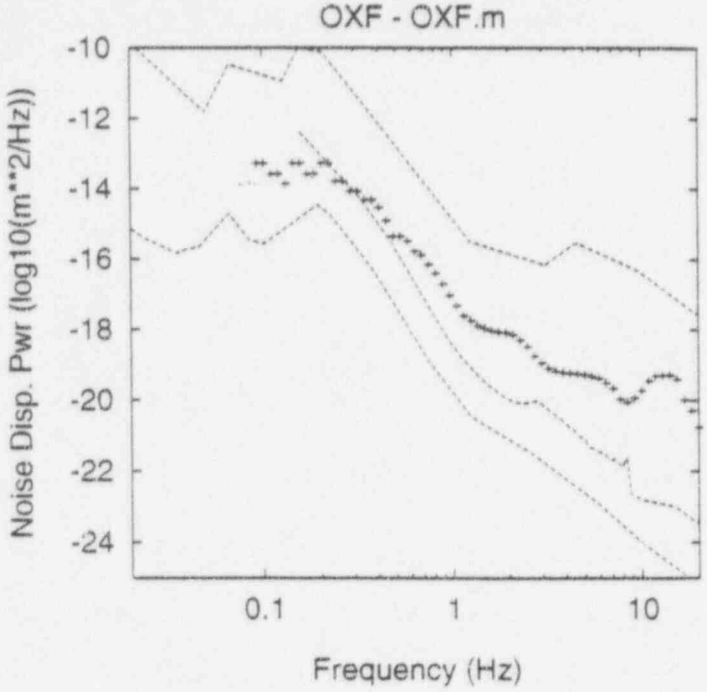

Figure 4.2m Spectral noise model for station OXF. Crosses show the smooth mean noise level. Dotted lines show the USGS high noise model, the mean GTSN day time noise level, and the USGS low noise model. OXF is a noisier than average station.

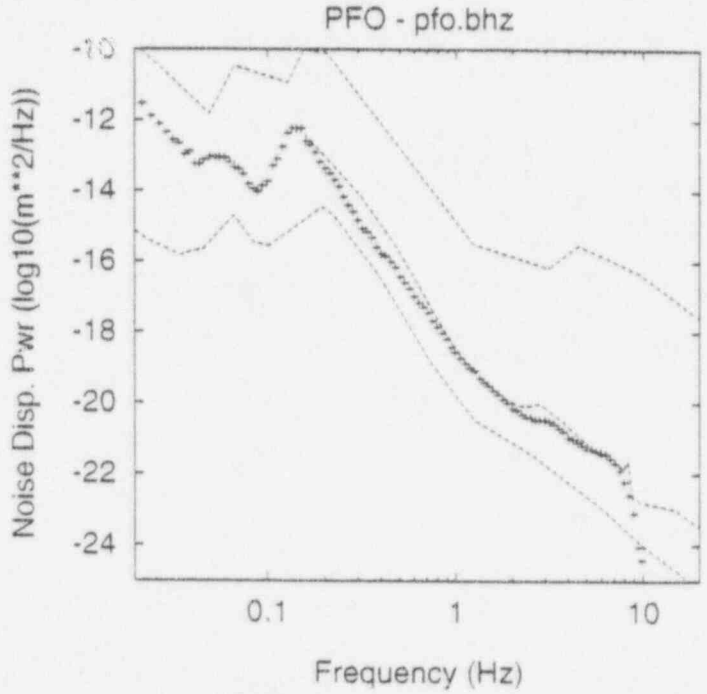

Figure 4.2n Spectral noise model for station PFO. Crosses show the smooth mean noise level. Dotted lines show the USGS high noise model, the mean GTSN day time noise level, and the USGS low noise model. PFO is an average station.

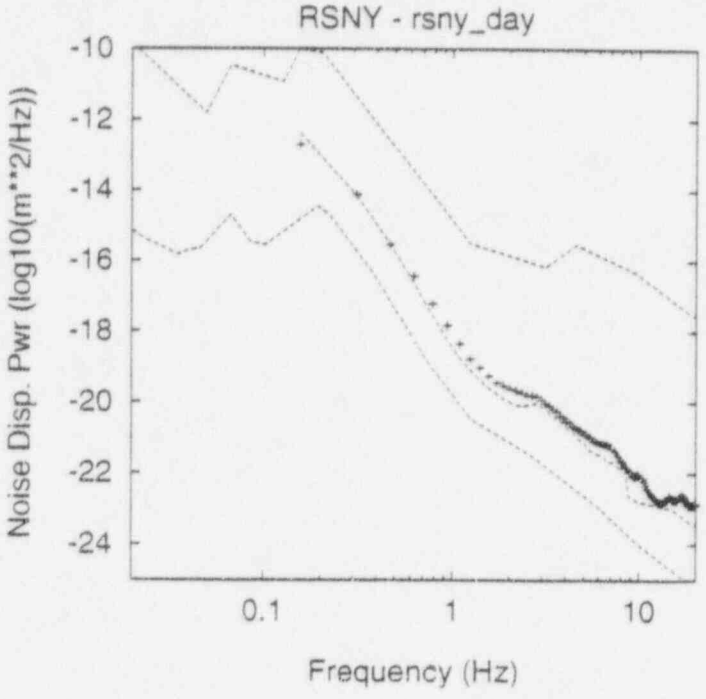

Figure 4.2o Spectral noise model for station RSNY. Crosses show the smooth mean noise level. Dotted lines show the USGS high noise model, the mean GTSN day time noise level, and the USGS low noise model. RSNY is an average station.

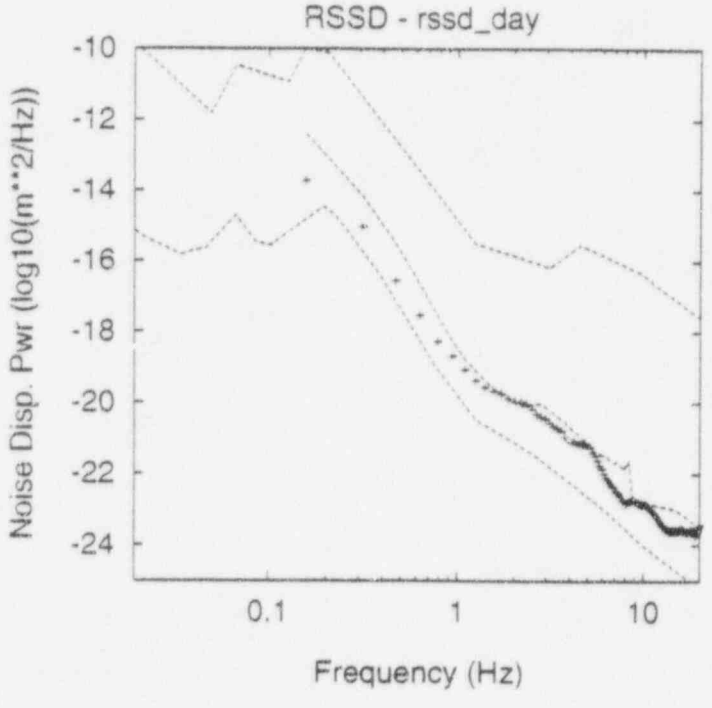

Figure 4.2p Spectral noise model for station RSSD. Crosses show the smooth mean noise level. Dotted lines show the USGS high noise model, the mean GTSN day time noise level, and the USGS low noise model. RSSD is a slightly quieter than average station.

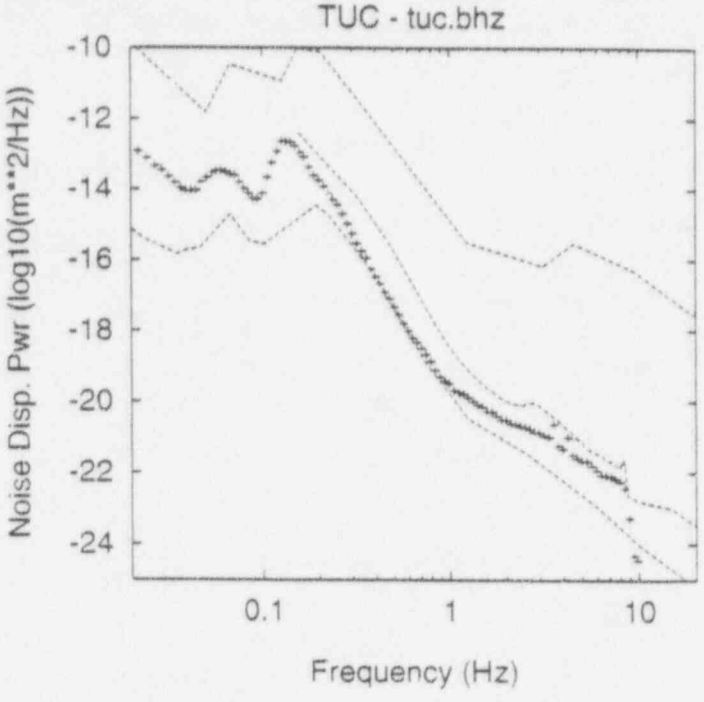

Figure 4.2q Spectral noise model for station TUC Crosses show the smooth mean noise level. Dotted lines show the USGS high noise model, the mean GTSN day time noise level, and the USGS low noise model. TUC is a quieter than average station.

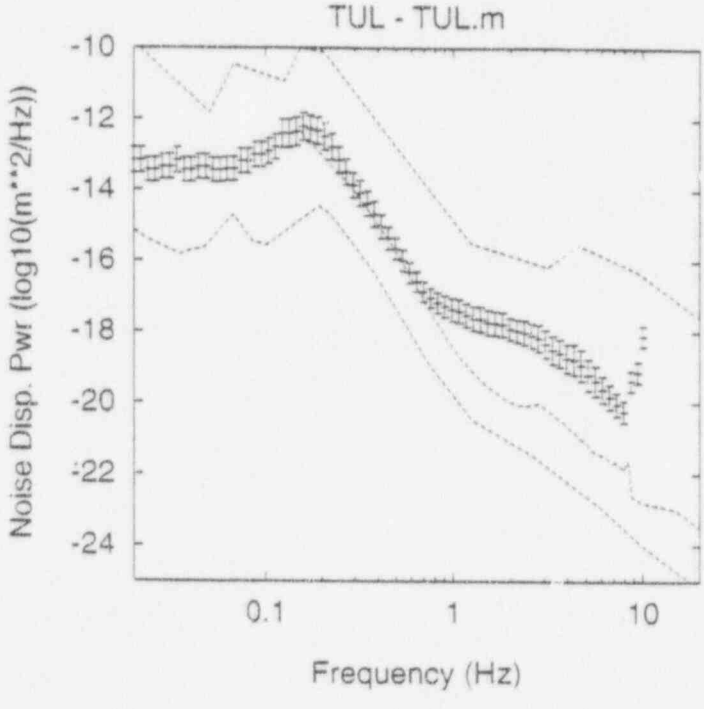

Figure 4.2r Spectral noise model for station TUL. Crosses show the smooth mean noise level. Dotted lines show the USGS high noise model, the mean GTSN day time noise level, and the USGS low noise model. TUL is a noisier than average station.

5.0 Preliminary Maps of Network Detection Capability

Figure 5.1 shows estimated contours of m_bLg for 90% probability of detection of 4 or more P waves by the currently operating USNSN stations. The 4 P-wave detection threshold is useful, since it usually requires 4 or more P waves to define and locate an event with assurance. However, since the USNSN does not operate entirely alone, in order to get a fair view of the detection threshold of the system we must include cooperating stations that are used in conjunction with the USNSN to detect earthquakes in the eastern US. Figure 5.2 shows estimated contours of m_bLg for 90% probability of detection of 4 or more P waves by the currently operating USNSN plus the real-time cooperative stations. Note that when compared to Figure 5.1, the detection levels are significantly improved in the central US, and along the eastern seaboard with the addition of the cooperating stations.

It should be noted that detection thresholds are not sharp cut-offs. There is a finite probability that small events will be detected below the 4 P-wave 90% detection threshold. Figure 5.3a,b illustrates this by showing USNSN plus cooperative stations detection probability contours for $m_bLg = 3.25$. Note that detection is 80% assured in much of the eastern US while it drops off virtually to zero toward the east in the Atlantic Ocean and toward the south in the Gulf of Mexico and Mexico. Because of a scarcity of stations in the upper Mid-west, the detection probability drops below 80% in a region of southern Indiana, Illinois, and western Kentucky. Figures 5.4,a,b demonstrate that the planned network of USNSN plus cooperative stations will fill this gap and the detection of $m_bLg = 3.25$ events will be 80% to 90% assured across much of the eastern US. The detection threshold will still be slightly higher than $m_bLg = 3.5$ along the Gulf of Mexico and in southwest Texas.

We should not consider the decline in detection capability to the north as realistic since the Canadian Geological Survey (CGS) operates the extensive Canadian National Seismic Network (CNSN) (North and Beverly, 1994; North 1994). Although US - Canadian cooperation is still informal, we can illustrate the potential benefits of this cooperation with detection probabilities for the USNSN plus cooperative US stations and the CNSN (Figure 5.5a). Figure 5.5b shows probability of 4 P detection at $m_bLg = 3.25$ for the combined US and Canadian networks. Probabilities of detection at $m_bLg = 3.0$ to 3.25 should be significantly higher in the northern US and southern Canada with close coordination of the USNSN and CNSN networks.

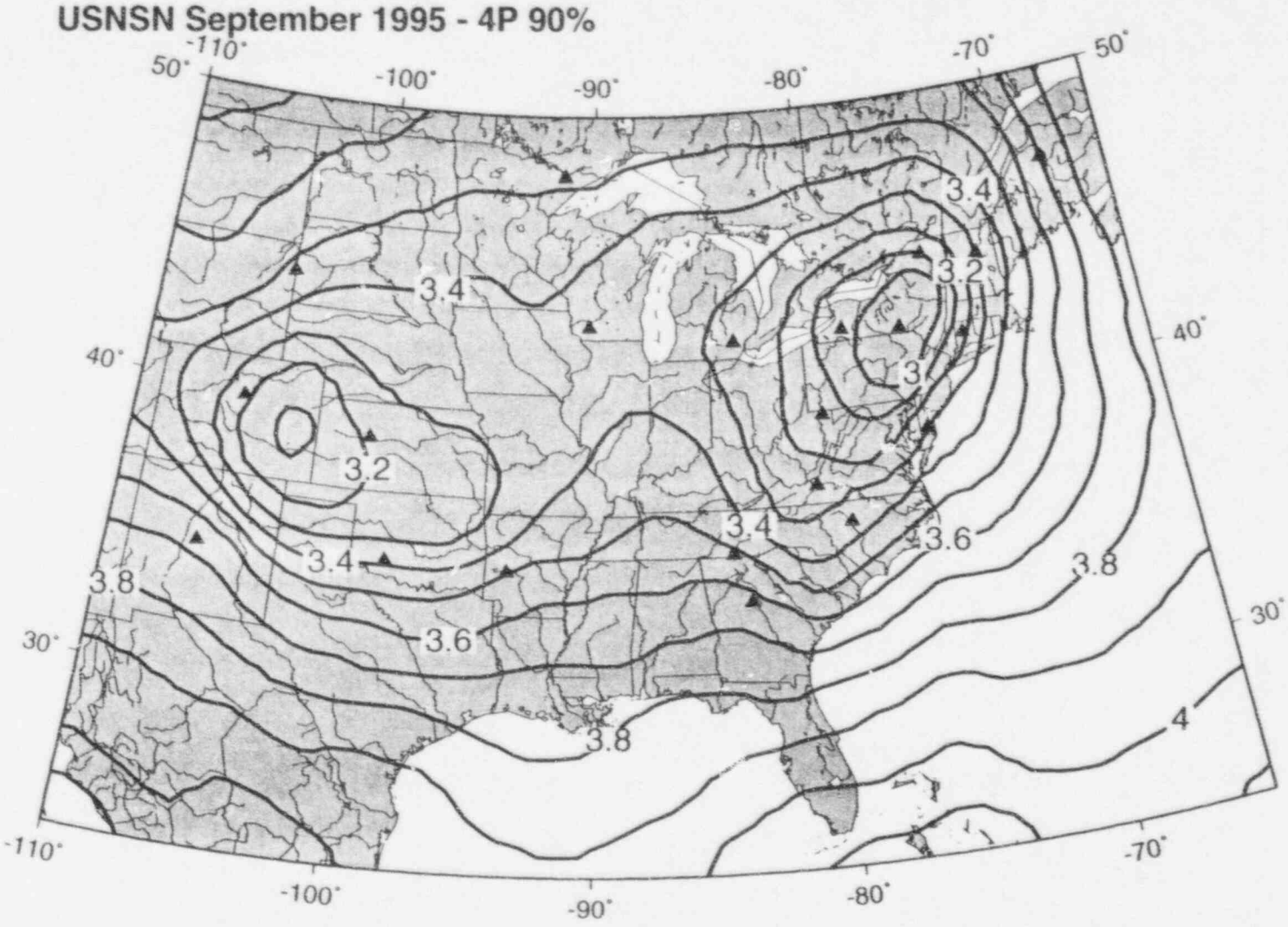

Figure 5.1 Estimated contours of m_bLg for 90% probability of detection of 4 P-waves at the USNS stations only.

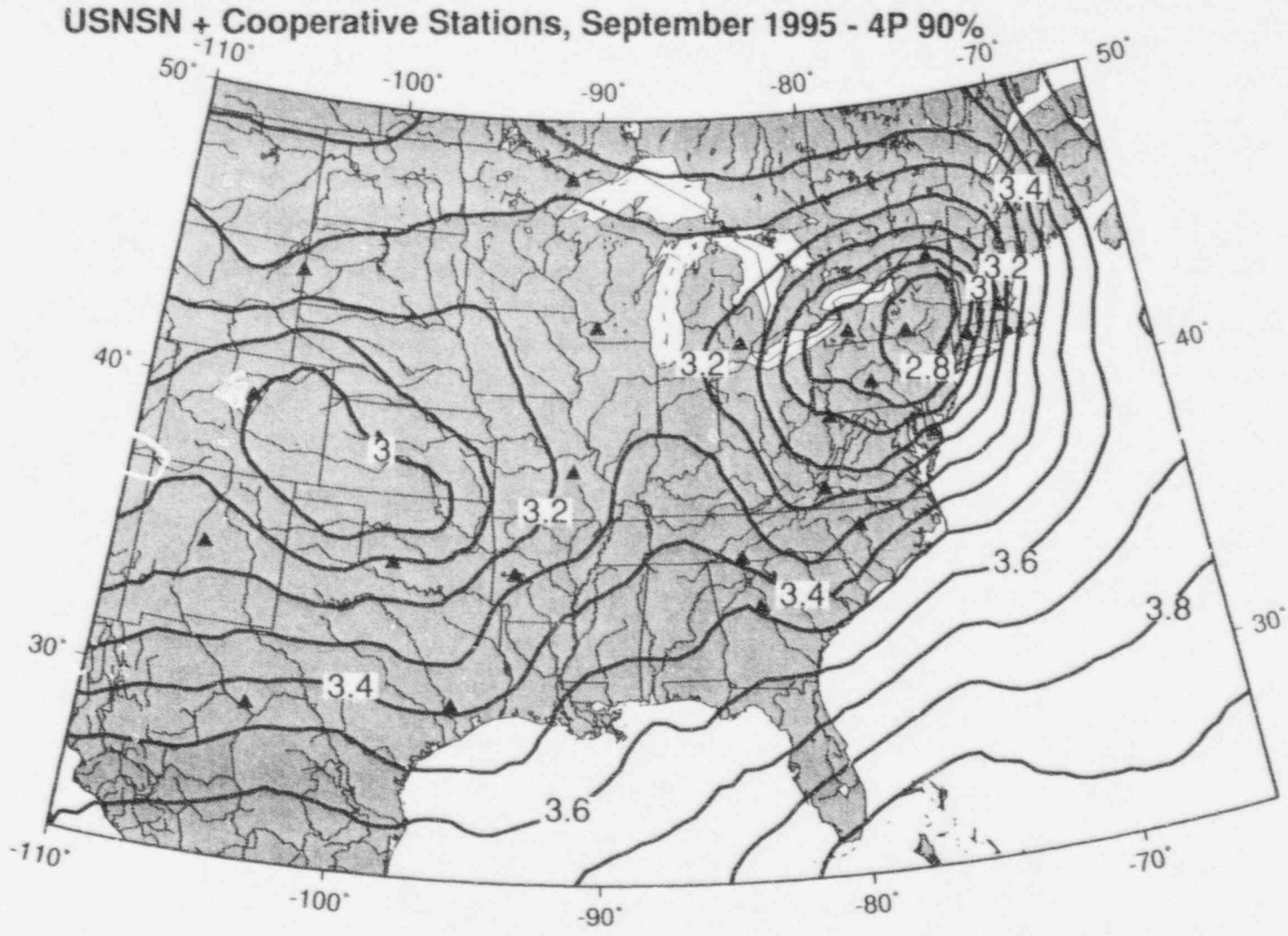

Figure 5.2 Estimated contours of m_bLg for 90% probability of detection of 4 P-waves at the USNS and real-time cooperative stations.

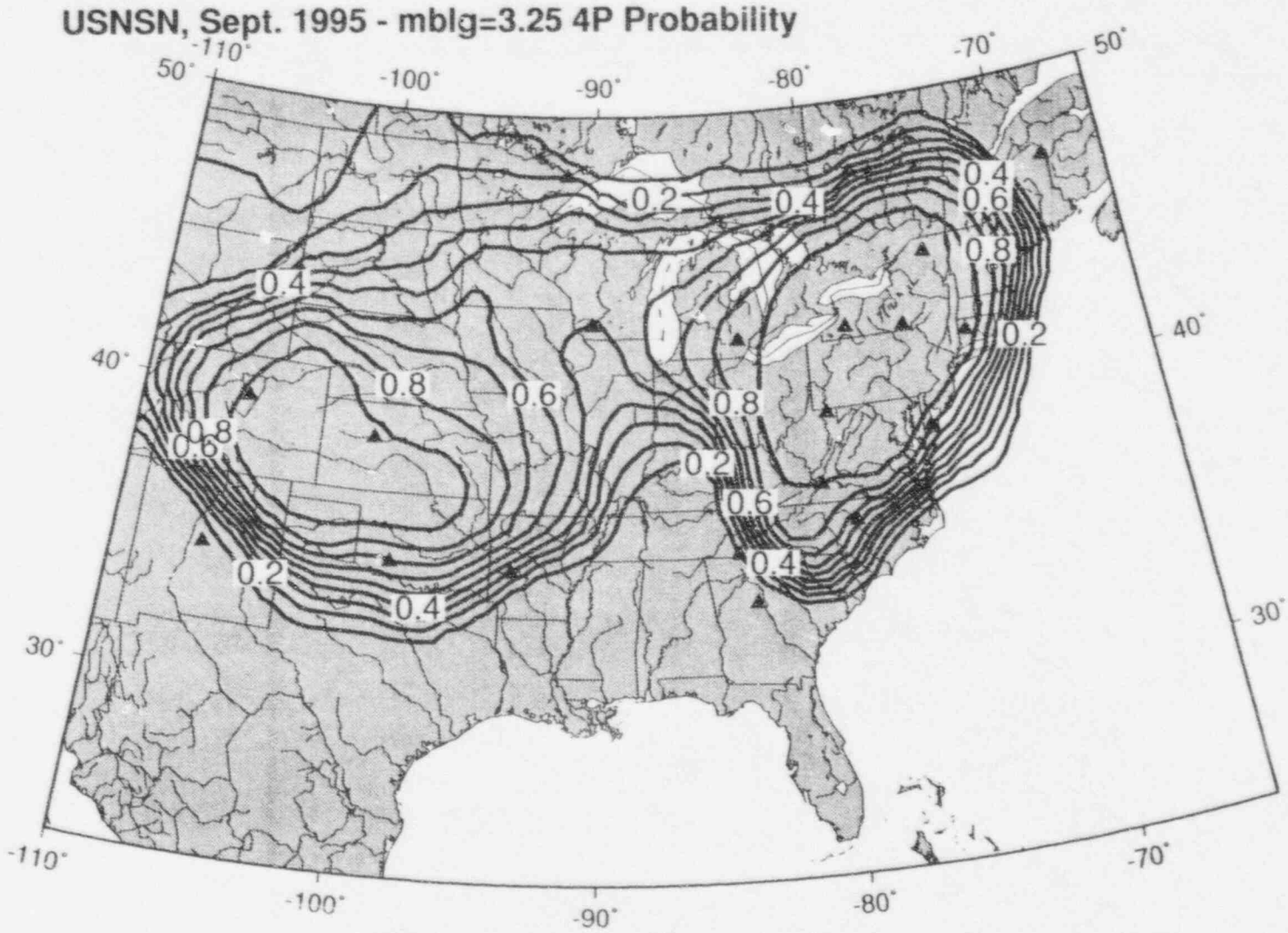

Figure 5.3a Probability of detection of 4 P-waves at USNS stations only for $m_bLg = 3.25$.

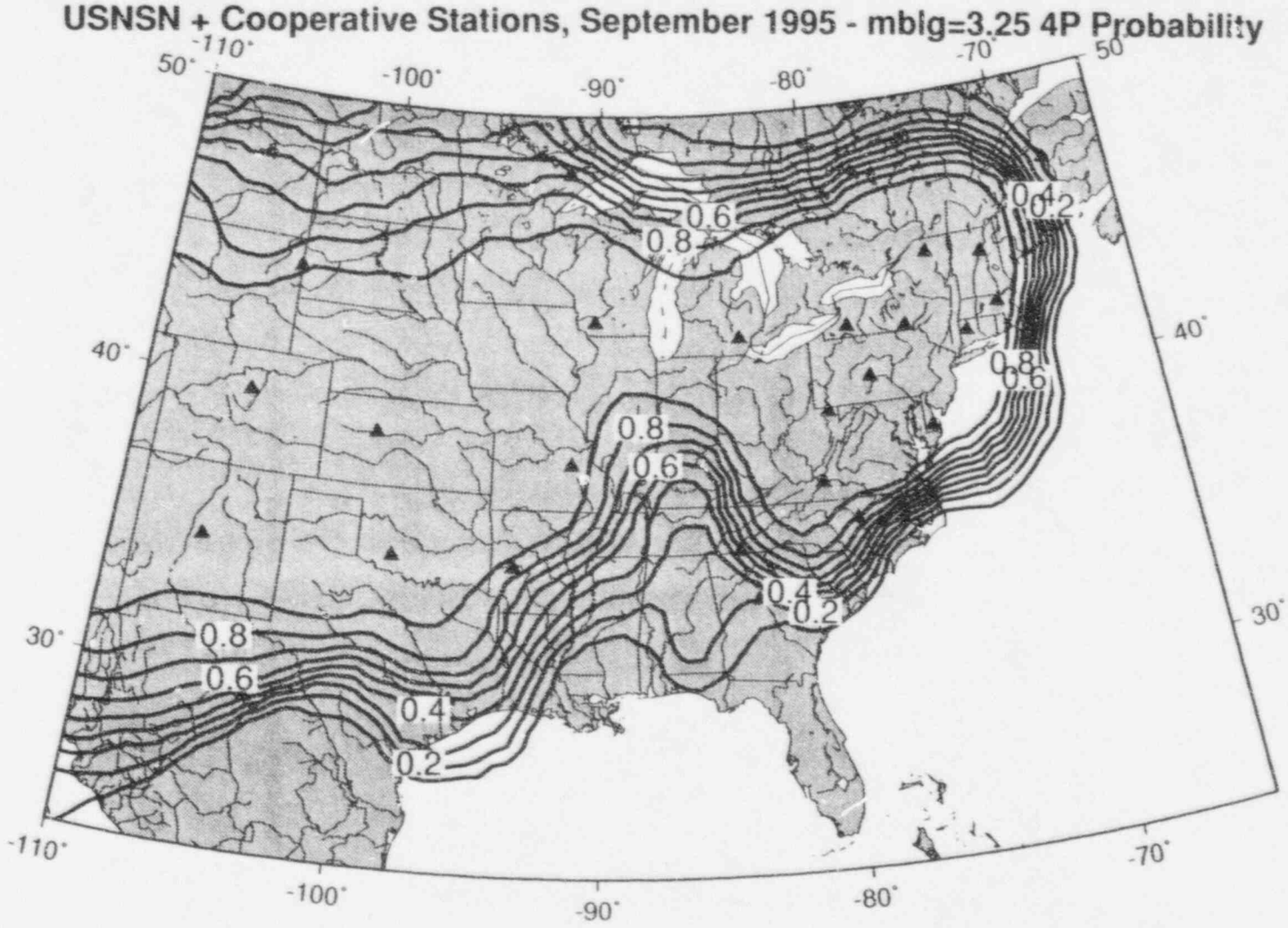

Figure 5.3b Probability of detection of 4 P-waves at USNS and real-time cooperative stations for m_bLg = 3.25.

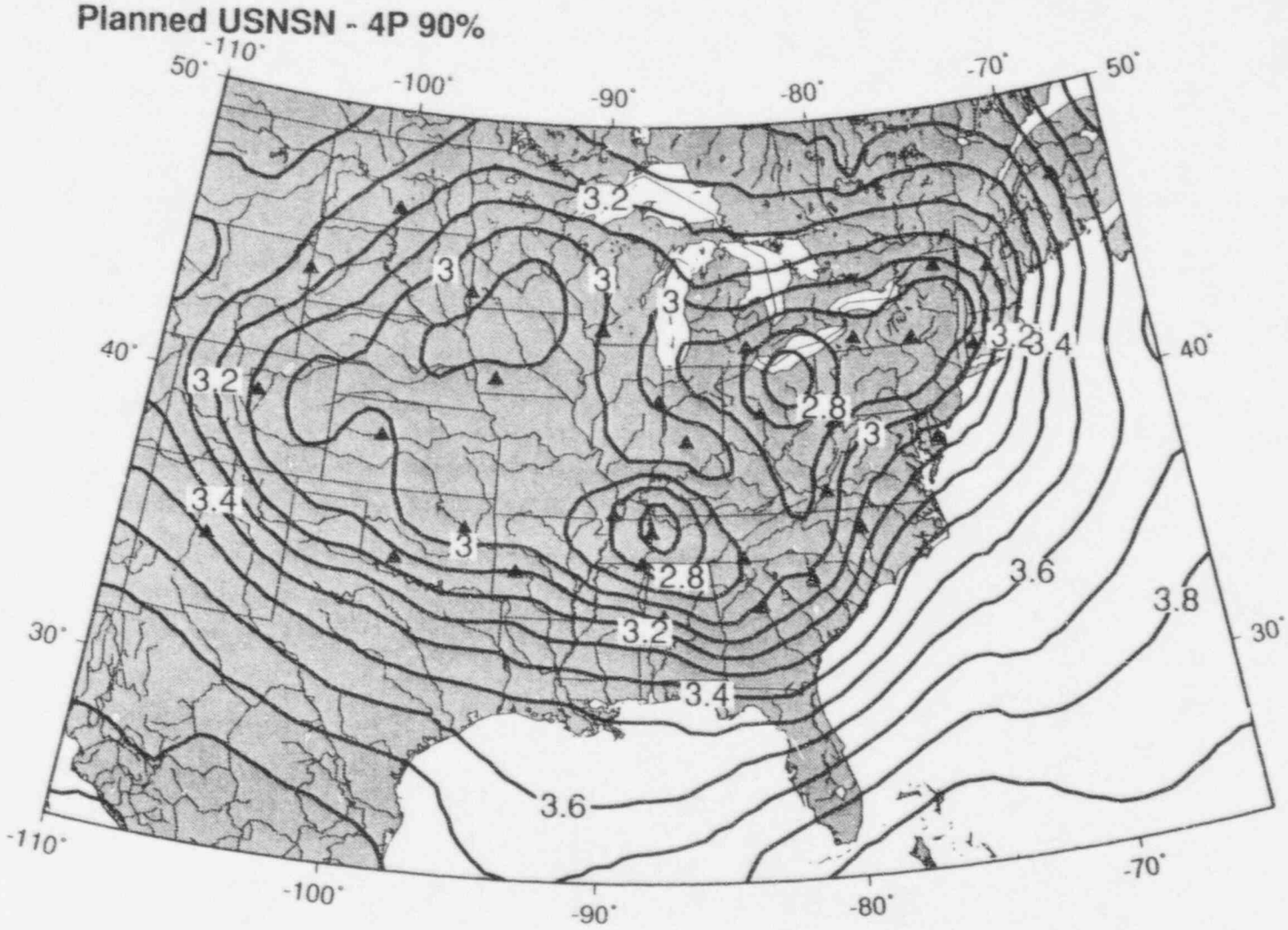

Figure 5.4a Estimated detection thresholds (90%) for 4 P-waves at planned USNS stations.

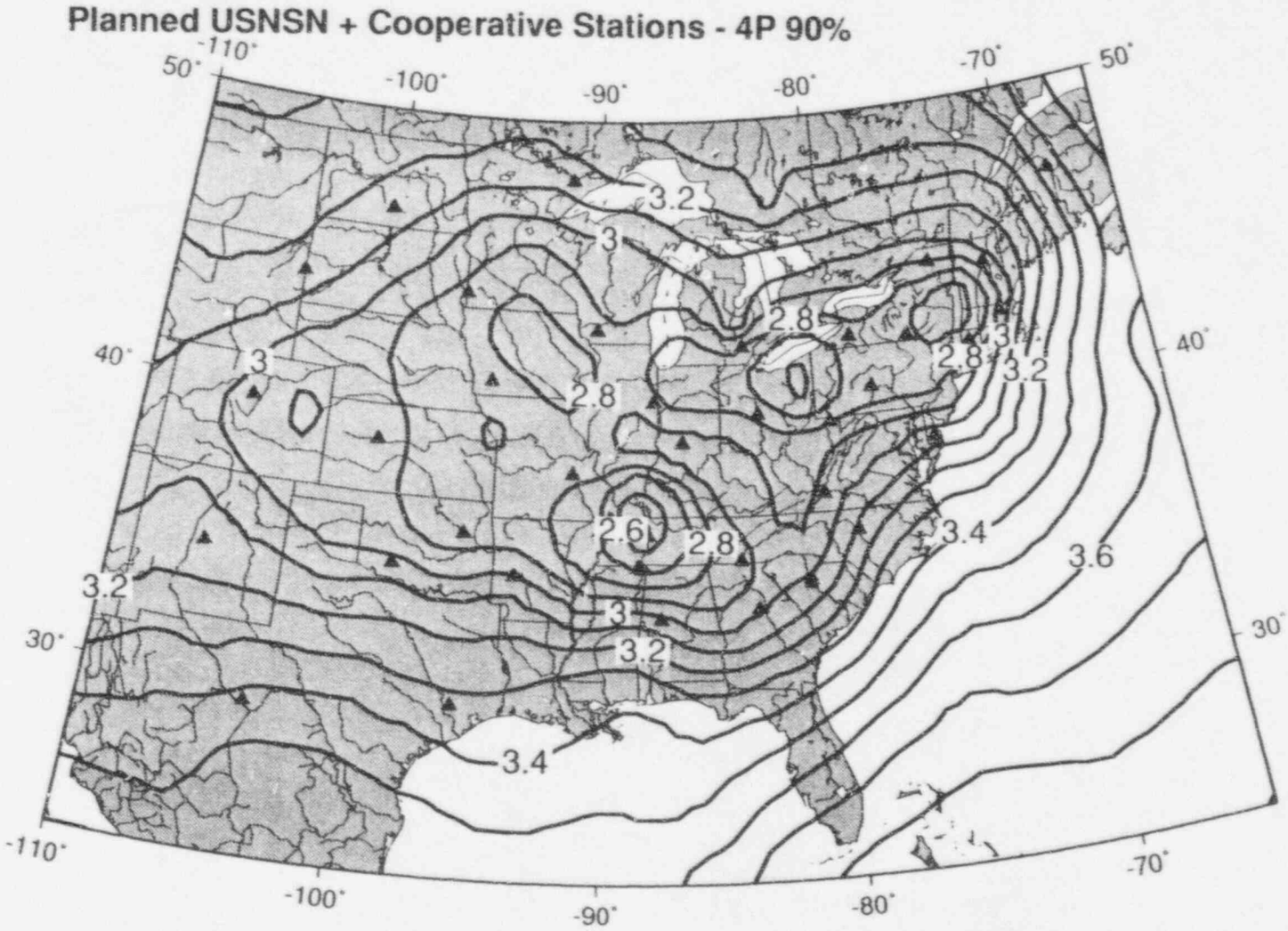

Figure 5.4b Estimated detection thresholds (90%) for 4 P-waves at planned USNS and cooperative stations.

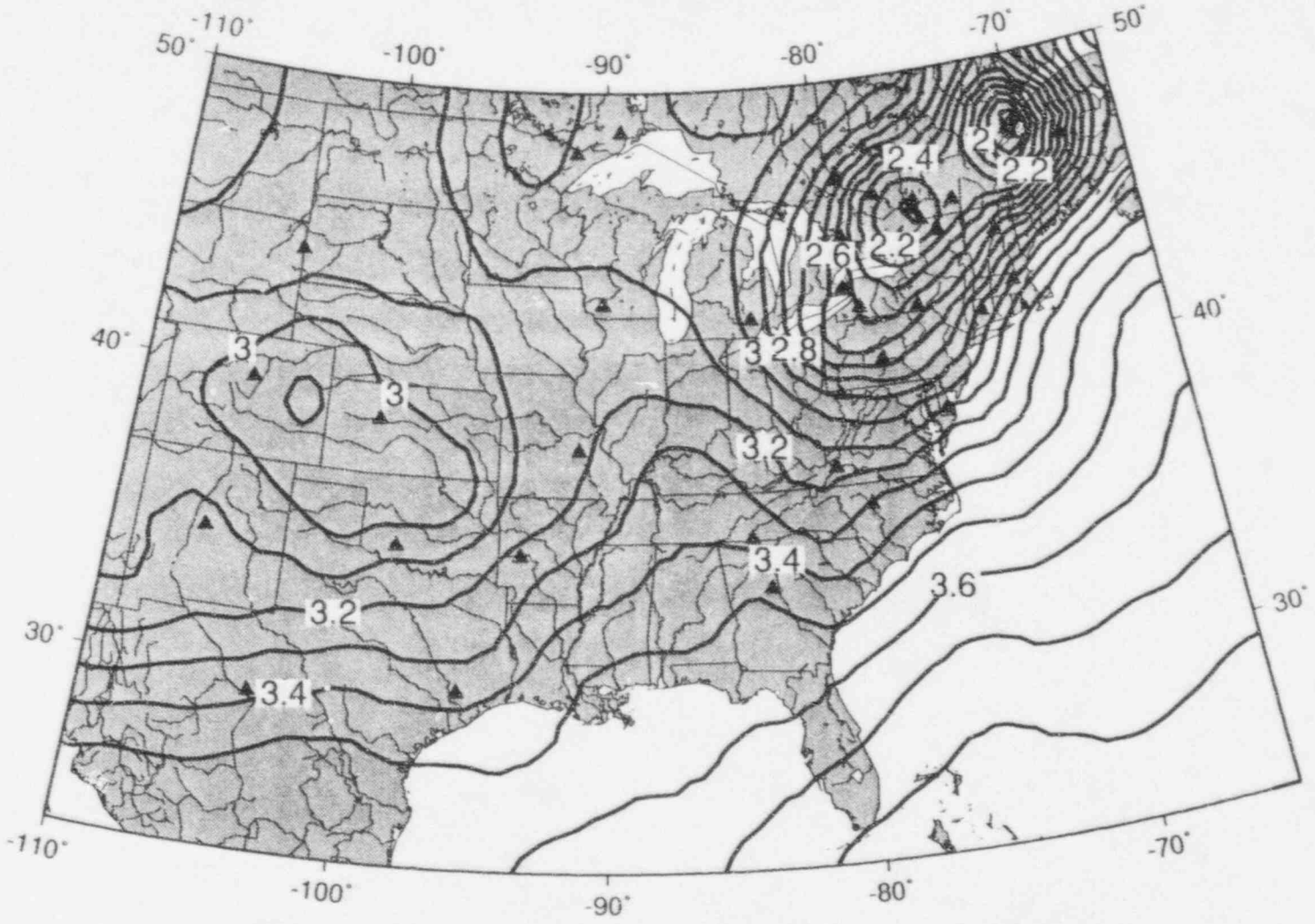

Figure 5.5a Estimated detection thresholds of combined USNSN, cooperative stations, and Canadian National Network for 90% detection of 4 P-waves.

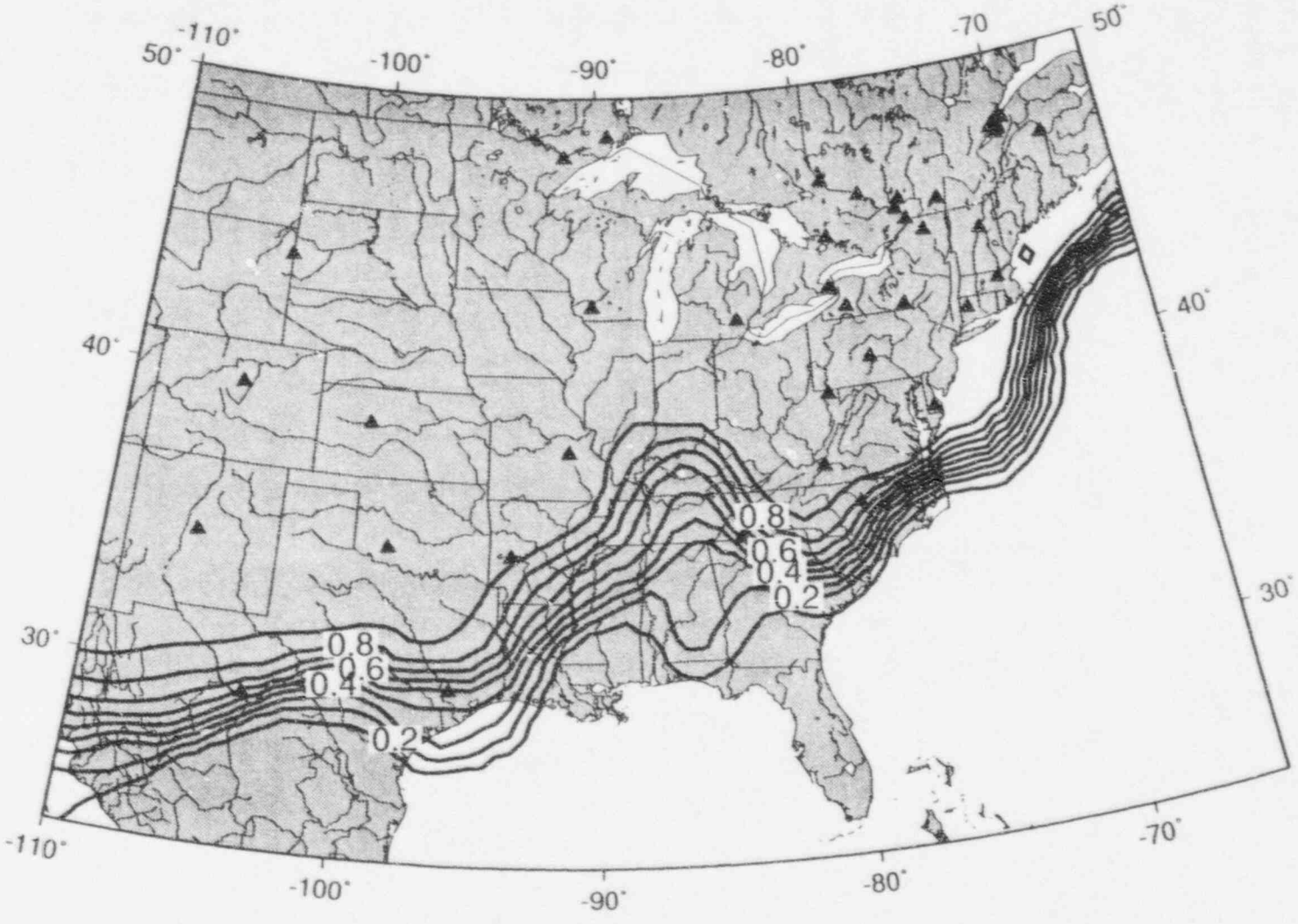

Figure 5.5b Probability of detection of 4 P-waves for USNS, cooperative stations, and Canadian National Network for 4 P-waves at $m_bLg = 3.25$.

6.0 Preliminary Maps of Network Location Capability

Once seismic phases are detected and associated to form an event with a preliminary location, the event must be located as precisely as possible. The precision with which an earthquake is located is often stipulated by a 90% probability error ellipsoid. Ninety percent of all true locations should be inside such ellipsoids provided all arrival errors are purely random and no important systematic errors exist. The ellipsoid is typically specified by it's semi-major axis, semi-minor axis and the azimuth (strike) of the semi-major axis.

In order to simulate the estimation of error ellipsoids, we use a Monte Carlo approach. At a given location we generate an ensemble of synthetic events with a specified magnitude (or moment). For each synthetic event we generate a set of phase arrivals at each station in the network. The amplitude of the phase and it's arrival time are given by deterministic models plus random terms. The synthetic noise level at the station is then predicted from the noise model plus a random term. The probability of detection at the station is then evaluated and a random number is selected from a uniform distribution from zero to unity. If the probability is greater than the random number the phase amplitude and arrival time are added to the synthetic event bulletin, otherwise the phase is discarded. Each event in the synthetic bulletin is then located using a standard location algorithm and the location and the estimated location precision is tabulated in the synthetic bulletin. Statistics are computed from the Monte Carlo synthetic bulletin to determine the 50% and 90% probability limits for the error ellipsoids in the synthetic bulletin. This procedure is then repeated for another location (latitude and longitude). Finally, the statistics can be contoured on a map to illustrate the location capability of the network for the fixed event size (magnitude or moment) as a function of location.

Figure 6.1a illustrates the location capability of the USNSN alone. Contours of the area (in square km) of the median (50% probability) ellipsoid are shown for a shallow magnitude $m_bLg = 3.5$ earthquake. We would expect that 50% of all shallow $m_bLg = 3.5$ earthquakes would have estimated locations better than the contours shown. Similarly, Figure 6.1b shows the contours of the 90% percentile ellipsoid area. Ninety percent of all $m_bLg = 3.5$ earthquakes should have locations better than contours shown.

As with the detection thresholds, it is unfair to consider the USNSN location capability without including the real-time cooperative stations. Figure 6.2a shows contours of the simulated median ellipsoid area for $m_bLg = 3.5$ while Figure 6.2b shows the 90% percentile contours for the USNSN plus cooperative stations. Note that location capability is much improved by the use of the cooperative stations. Obviously, earthquake locations are expected to improve for larger events as illustrated by the simulated 50% and 90% percentile ellipsoid areas shown in Figures 6.3a and 6.3b for $m_bLg = 4.5$ located by the USNSN plus cooperative stations.

While the area of the location ellipsoid provides a good indication as to how well the event is located, it is often the case because of network geometry, the ellipsoid becomes elongated and the location uncertainty is better described by the semi-major axis. Figures 6.4a,b show predicted contours for the 90 percentile semi-major axis for the USNSN plus cooperative stations at m_bLg = 3.5 and 4.5 respectively.

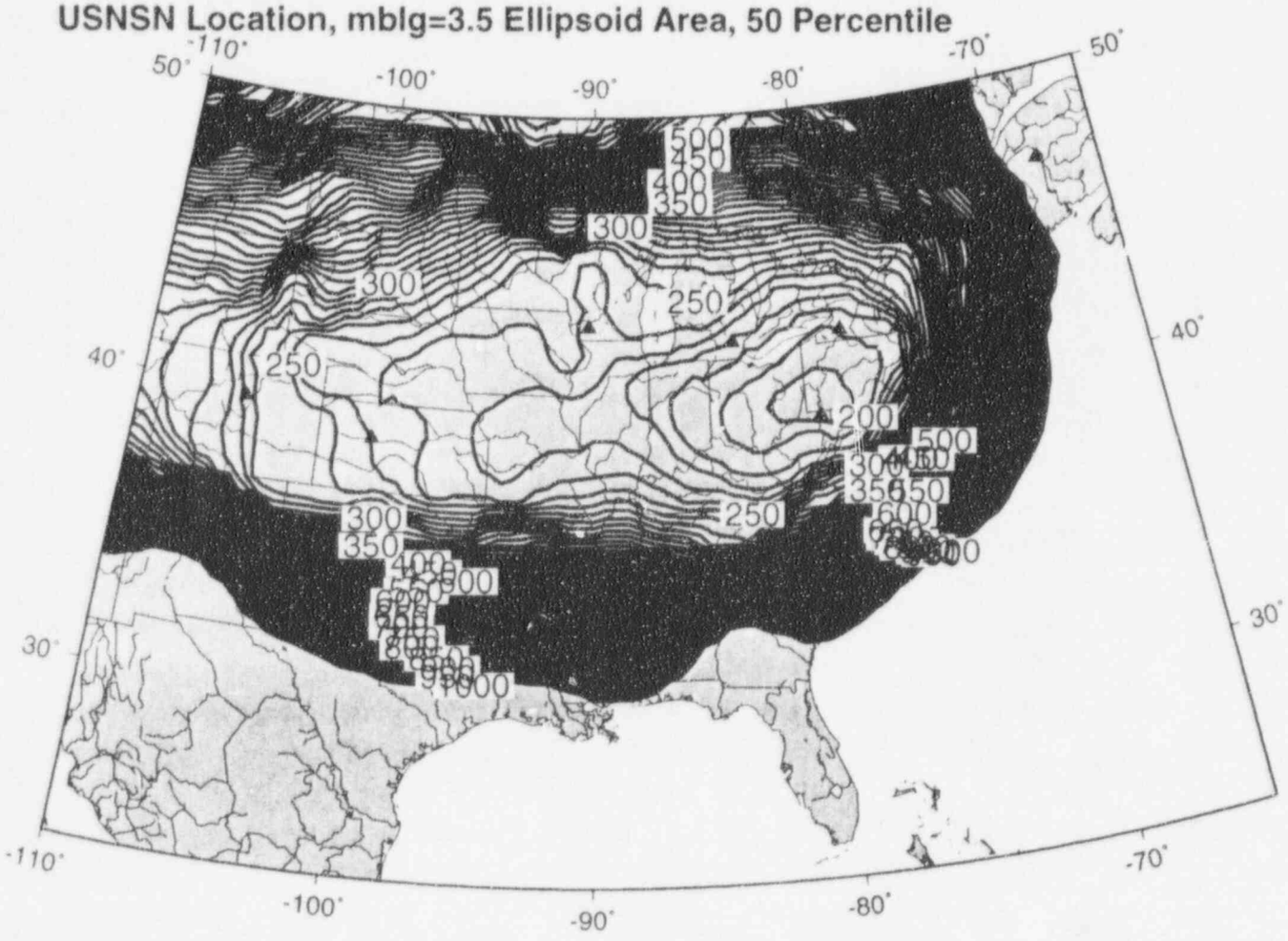

Figure 6.1a Contours of 50 percentile location ellipsoid area (square km) for m_bLg=3.5 detected by the USNSN. Note that location capability of the USNSN quickly degrades around the periphery of the network and is best (about 200-250 square km) in the center of the network.

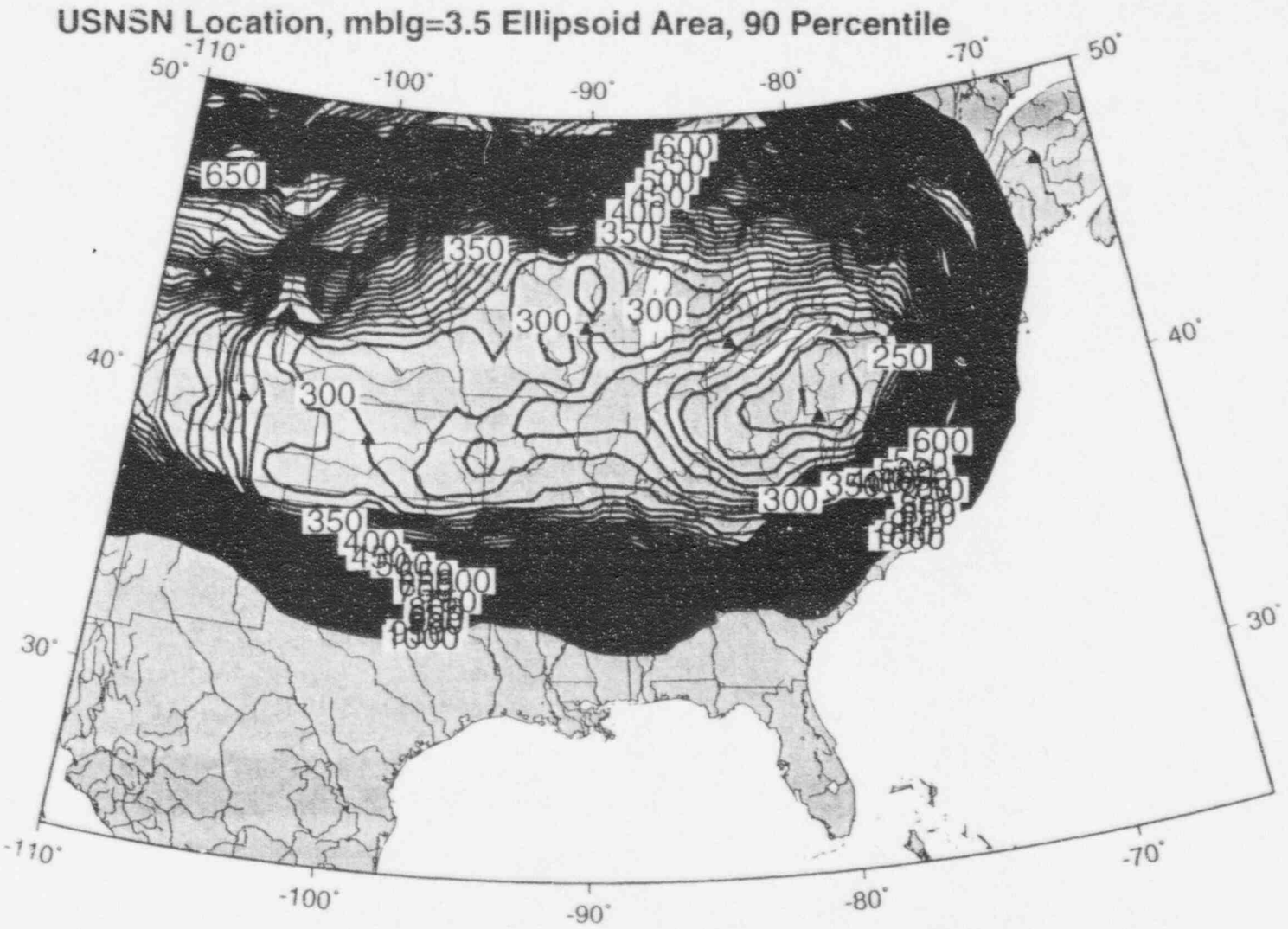

Figure 6.1b. Contours of 90 percentile location ellipsoid area (square km) for m_bLg=3.5 detected by the USNSN. Note that location capability of the USNSN quickly degrades around the periphery of the network and is best (about 250-300 square km) in the center of the network.

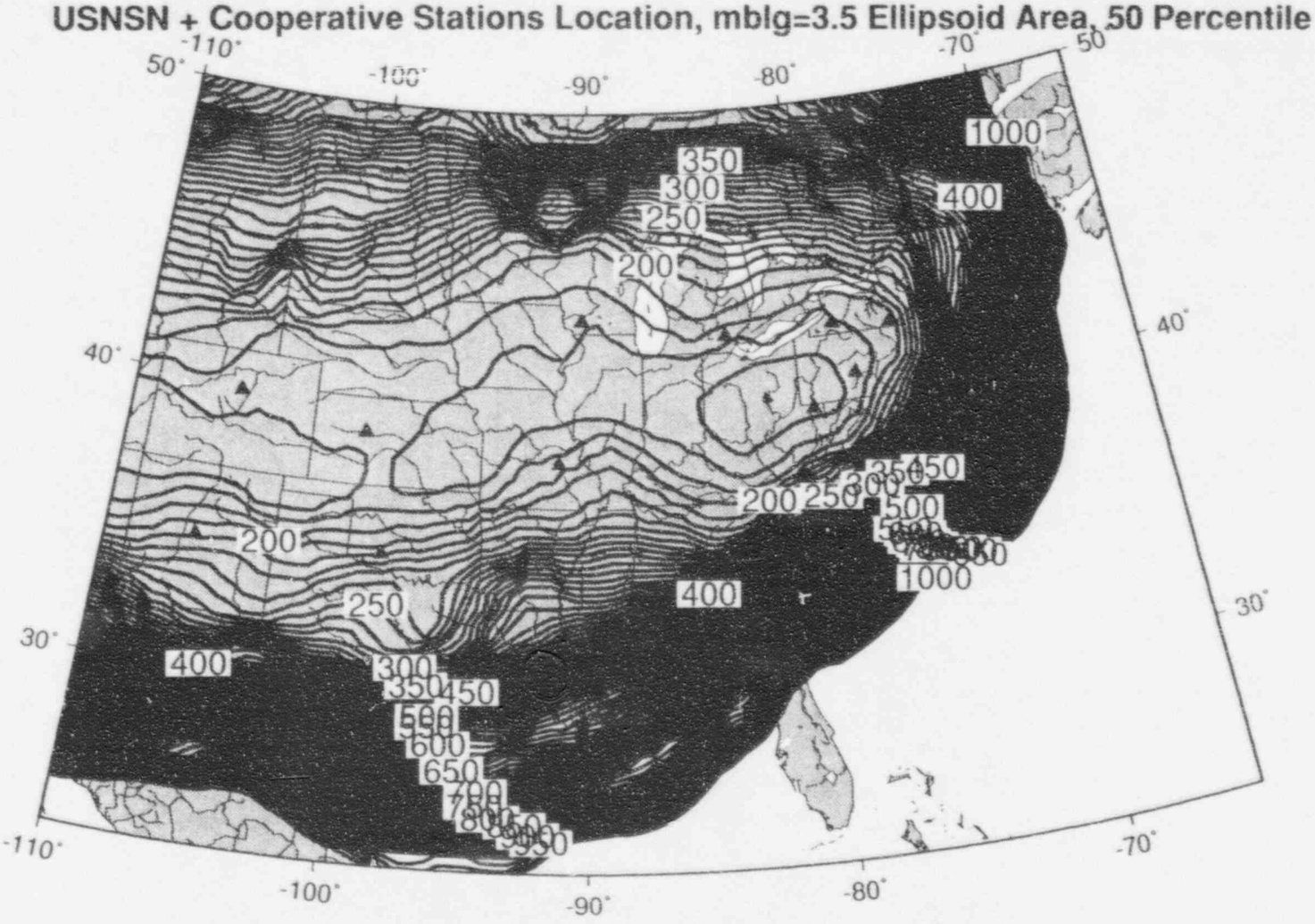

Figure 6.2a. Contours of 50 percentile location ellipsoid area (square km) for m_bLg=3.5 detected by the USNSN and real-time cooperative stations. Note that location capability of the network is more extensive than that shown in Figure 6.1a.

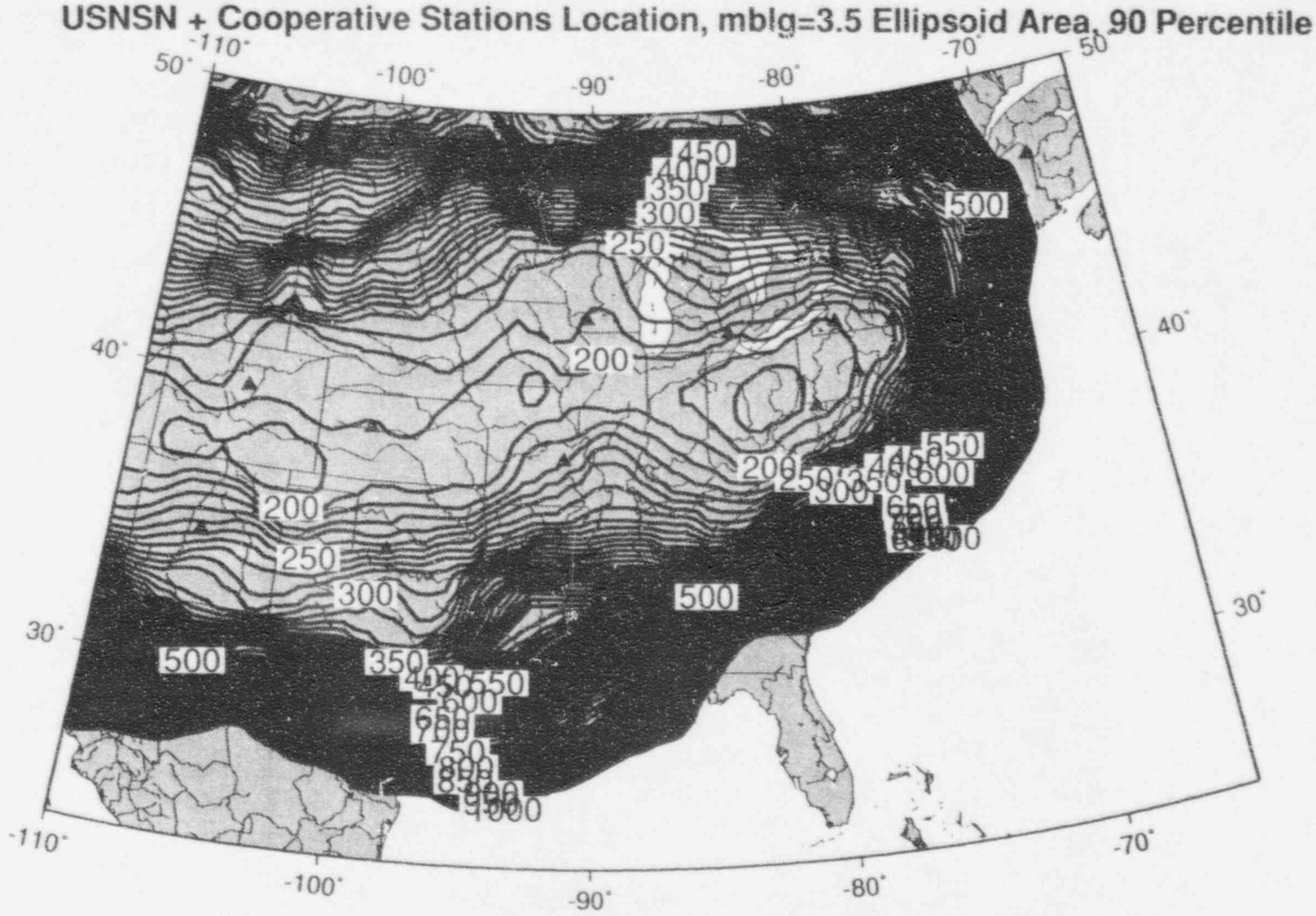

Figure 6.2b. Contours of 90 percentile location ellipsoid area (square km) for m_bLg=3.5 detected by the USNSN and real-time cooperative stations. Note that location capability of the network is more extensive than that shown in Figure 6.1b.

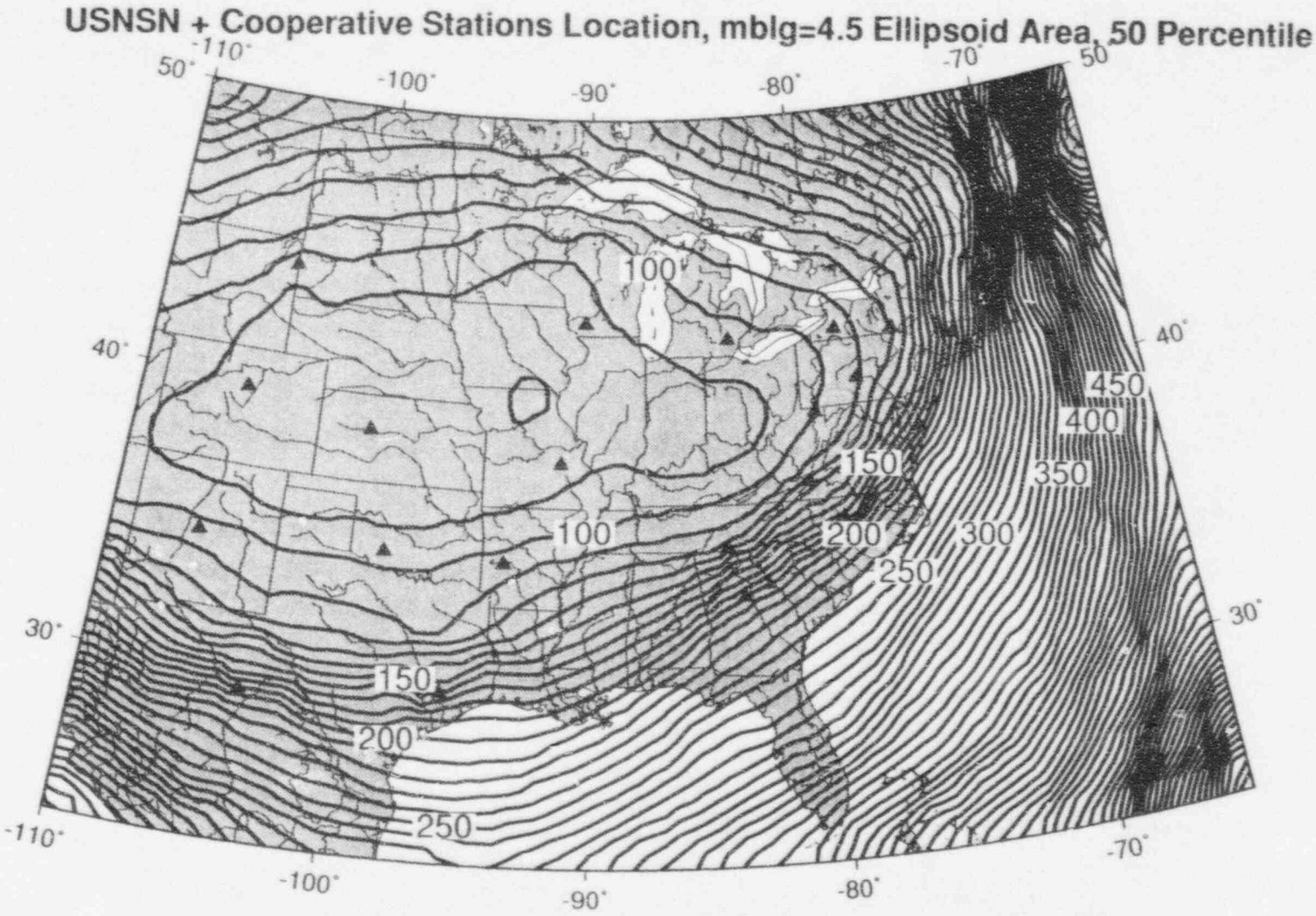

Figure 6.3a. Contours of 50 percentile location ellipsoid area (square km) for m_bLg=4.5 detected by the USNSN and real-time cooperative stations. Note that location capability of the network is better than that shown in Figure 6.2a.

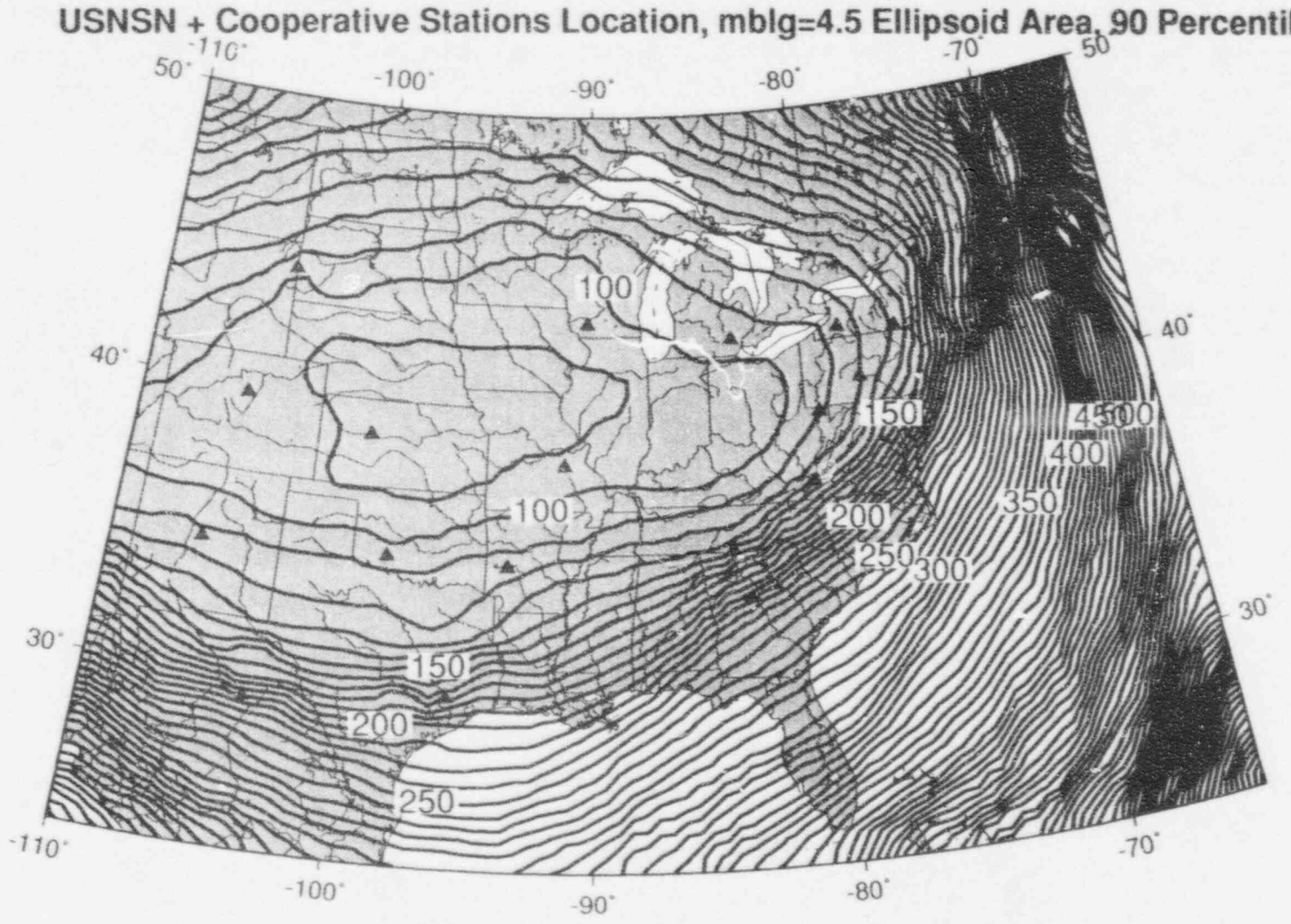

Figure 6.3b. Contours of 90 percentile location ellipsoid area (square km) for m_bLg=4.5 detected by the USNSN and real-time cooperative stations. Note that location capability of the network is better than that shown in Figure 6.2b.

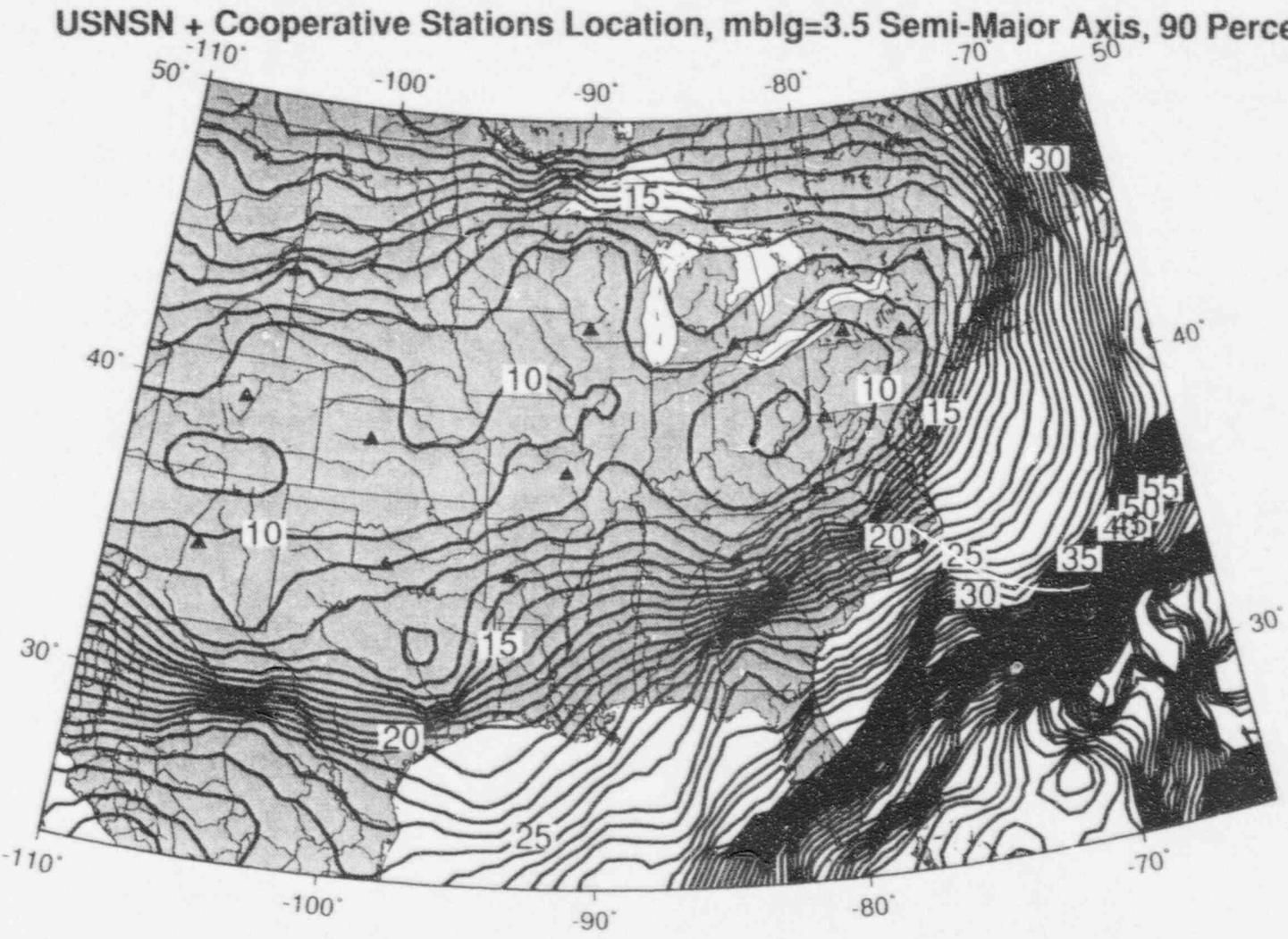

Figure 6.4a. Contours of 90 percentile semi-major axis (km) for m_bLg=3.5 detected by the USNSN and real-time cooperative stations.

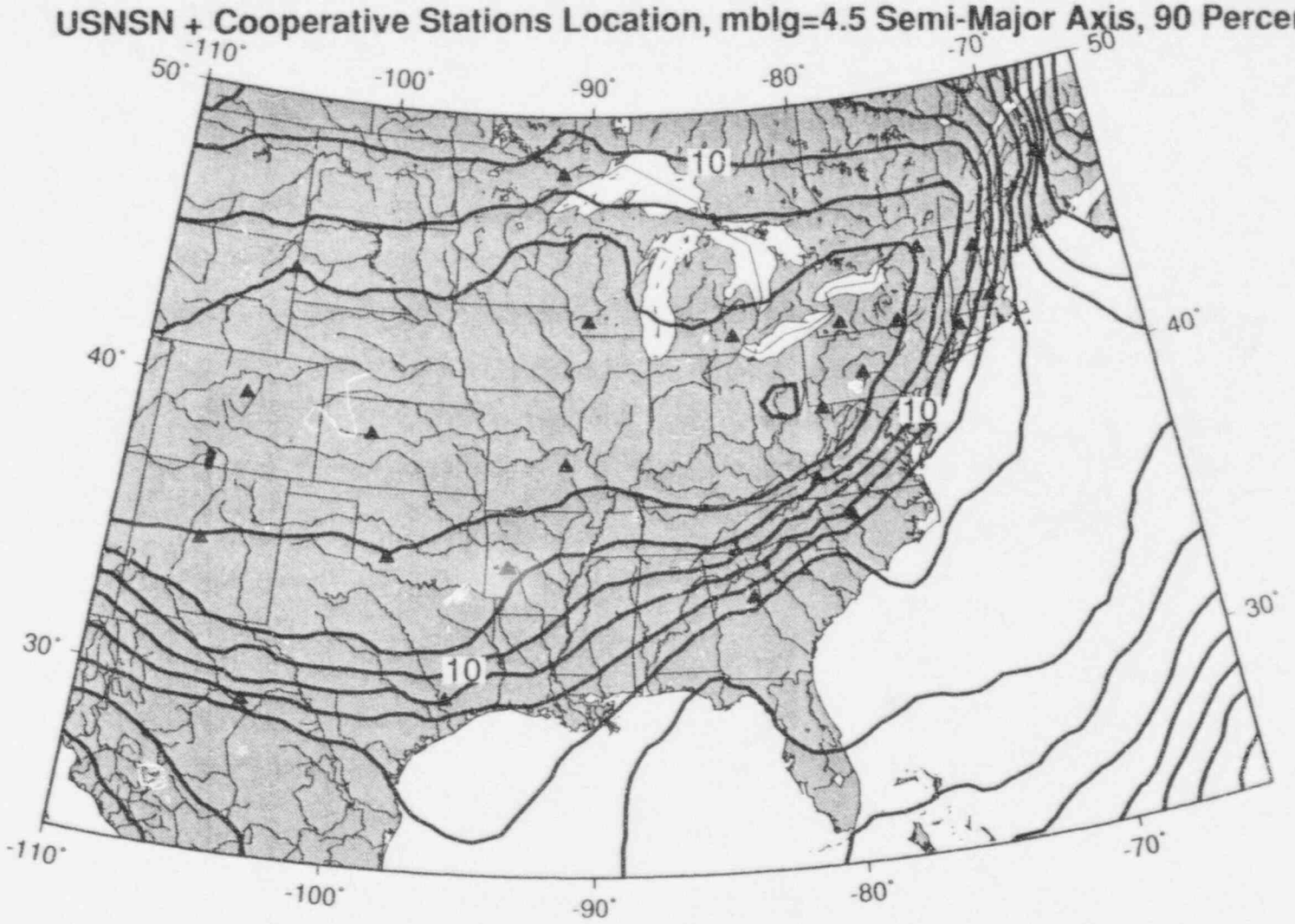

Figure 6.4b. Contours of 90 percentile semi-major axis (km) for m_bLg=4.5 detected by the USNSN and real-time cooperative stations.

7.0 Ground Truth Comparisons of Location Capability

There are two components to the location uncertainty, systematic and random. We can model the random component of uncertainty with Monte Carlo methods as described above but the systematic errors are much more difficult to model. Systematic location errors occur for two reasons. First, the laterally averaged crustal velocity structure may not be properly known and therefore predicted travel times may be systematically incorrect as a function of distance or phase. Second, the Earth is laterally heterogeneous and the use of laterally averaged velocity structures lead to systematically incorrect predicted travel times as a function of distance and azimuth for any location and phase.

In order to gain insight into these two types of errors we are using events for which locations are known to high precision and accuracy and we can use this information as "ground truth." Several large industrial related events with magnitudes 2 to 4 occur each year in the US. These include large blasts at the magnitude 2 to 3 level and occasional mine collapses, bumps, or rockbursts that can reach the magnitude 5 level. Additional event locations are available for well located events within tight networks where one or more stations are located nearly on top of the event(s).

The tables below (Tables 7.1 and 7.2) list some of the industrial event locations that have been collected so far under this project and will be more closely studied in the second year of the effort. Figures 7.1 and 7.2 show the ground truth (GT) locations for the Kentucky and Wyoming mine collapses and some locations determined by the USGS, VPI, and the GSETT-3 IDC. Error ellipses are not available at this time for the USGS locations.

Table 7.1 95/03/11 Lynch Mine Bumps -Eastern Kentucky

Source	O.T.	Lat.	Long.	H	E1	Az1	E2	Az2		Magnitude
Lynch Mine	08:15:53.00	36.9322	-83.0253	0.0	~2.	0	~2.	90	Ground Truth	
IDC	08:15:53.74	36.84720	-82.8513	0.0	16.8	155	10.7	245	H Fixed	4.1 m_b
VPI	08:15:53.98	36.96483	-83.0745	0.01	2.41	273	3.59	3.	H Fixed	
USGS 1	08:15:52.00	36.983	-83.15	0.0	-	-	-	-	H Fixed	3.6 m_b 3.8 m_bLg
USGS 2	09:50:04.40	36.99	-83.18	0.0	-	-	-	-	H Fixed	3.3 m_bLg

Table 7.2 95/02/03 Rockburst - Southwestern Wyoming

Source	O.T.	Lat.	Long.	H	E1	Az1	E2	Az2		Magnitude
IDC	15:26:16.00	41.62	-109.7600	24.7	20.6	72	13.7	162.	H Free	5.0 m_b
USGS	15:26:16.00	41.527	-109.6390	1.0	-	-	-	-	H Fixed	5.2 m_b 4.6 M_s
U.S. Bureau of Mines	15:26:16.00	41.4885	-109.785	1.0	1.1	0	0.45	90.	Ground Truth	
PWNA	15:26:12.9	41.5183	-109.8083	4.0					H Fixed	5.1 M_L 4.8 M_W

Depths (H) are in km
E1 is the 90% semi-major axis in km
Az1 is the azimuth of E1
E2 is the 90% semi-minor axis in km
Az2 is the azimuth of E2
PWNA is Pechmann, *et al.* (1995).

The errors in the USGS locations (Tables 7.1 and 7.2) relative to ground truth are consistent with the errors projected for the USNSN in these two regions. Furthermore, ellipses for the IDC locations are consistent with errors projected for the GSETT-3 network. Comparisons such as these are important checks on the projected location capabilities derived from network simulations.

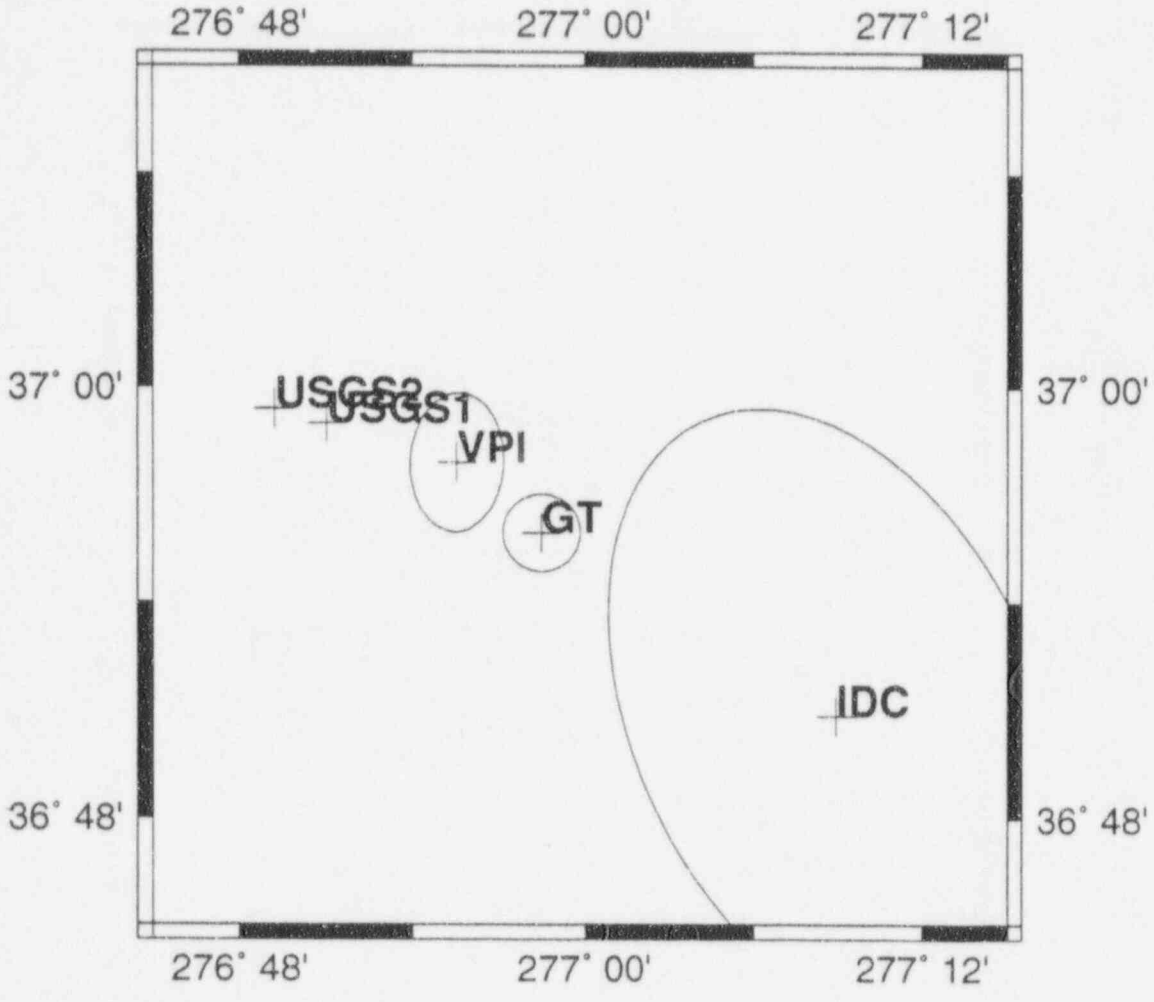

Figure 7.1 Map of locations for the 95/03/11 Lynch Mine bumps in eastern Kentucky. GT (ground truth) indicates the location and general spatial extent of the mine workings. VPI indicates VPI location with 90% error ellipse based on a regional network of about 50 detecting stations. IDC indicates a location from the GSETT-3 IDC with a 90% error ellipse. USGS1 and USGS2 indicate the USGS locations for the principal event (3.8 m_bLg) and a smaller event (3.3 m_bLg). No error ellipses are available for the USGS locations.

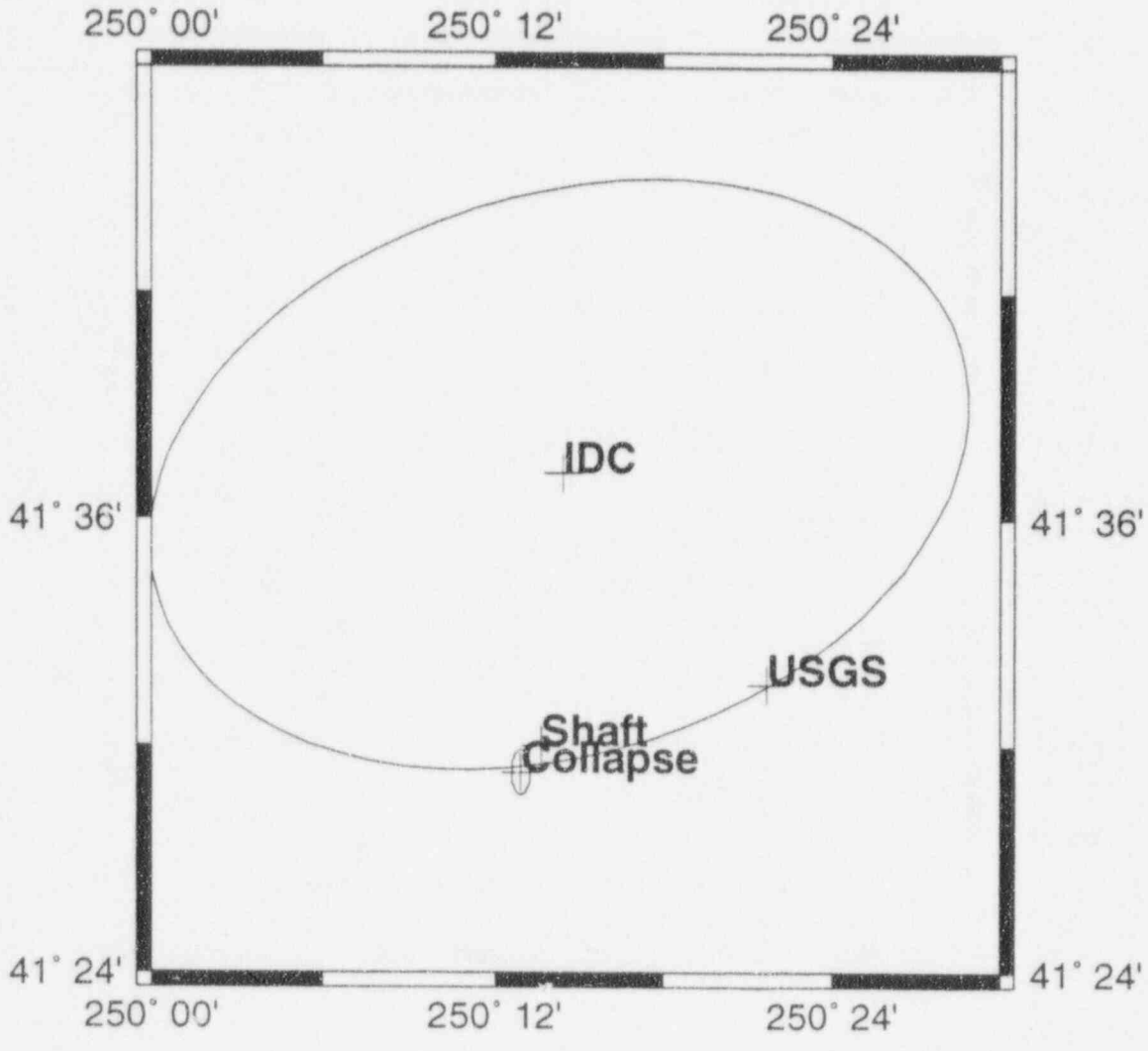

Figure 7.2 Map of locations for the 95/02/03 rockburst in southwest Wyoming. The shaft collapse indicates the region of underground collapse provided by the U.S. Bureau of Mines and Pechmann, *et al.* (1995). IDC indicates a location from the GSETT-3 IDC with a 90% error ellipse. USGS indicates the USGS location for the principal event. No error ellipses are available for the USGS locations.

8.0 Regional Attenuation (Lg, S, and Coda Q(f)) Models

In order to model regional wave propagation as a function of distance and frequency, we have begun to collect regional Q estimates for the EUS. Some of these are tabulated below. In each case we have interpreted the author's results in the form of $Q(f) = Q(f=1)f^{\zeta}$.

Table 8.1 Lg and S-Wave Attenuation Values

Locality	Q (1 Hz)	ζ	Wave Type	Reference
Northeastern US	590	0.35	Lg	Ebel (1995)
Eastern Canada	670	0.33	S	Atkinson and Mereu (1992)
Eastern Canada	900	0.20	Lg	Hasegawa (1985)
Northeastern US	525	0.65	Lg	Shin and Herrmann (1987)
Miss. Embayment	900	0.40	Lg	Singh & Herrmann (1983)
Central US	1200	0.20	Lg	Singh & Herrmann (1983)
Southern Appalachia	1000	0.10	Lg	Singh & Herrmann (1983)
Eastern and Central U.S.	900	0.00	Lg	Street (1976)
Eastern Canada	1100	0.19	S/Lg	Chun, *et al.* (1987)
Eastern and Central U.S.	800	0.32	Lg	Gupta & McLaughlin (1987)
Central U.S.	1500	0.3	Lg	Nuttli (1981)
Eastern U.S.	800	0.5	Lg	Nuttli (1981)
Eastern and Central U.S.	1000	0.35	Lg	Goncz & Dean (1986)
Rocky Mt. Front	880	0.23	Lg	Gupta & McLaughlin (1989)
Superior Shield	950	0.40	Lg	Gupta & McLaughlin (1989)
Midwest and Plains Platform	950	0.37	Lg	Gupta & McLaughlin (1989)
Eastern Canadian Shield and Greenville Province	1690	0.39	Lg	Gupta & McLaughlin (1989)
Appalachian Plateau and Fold Belt	1430	0.15	Lg	Gupta & McLaughlin (1989)
Atlantic Coastal Plain	600	0.40	Lg	Gupta & McLaughlin (1989)
Upper Miss. Embayment	920	0.33	Lg	Gupta & McLaughlin (1989)
Lower Miss. Embayment	550	0.73	Lg	Gupta & McLaughlin (1989)
Gulf Coastal Plain	200	0.93	Lg	Gupta & McLaughlin (1989)

9.0 Eastern U.S. Site Conditions

It has been noted that local station amplitudes are correlated with shallow geology (Gupta, *et al.*, 1989) even for regional seismic phases such as Lg. In order to evaluate this possibility in the future, we have made a preliminary characterization of the USNSN station sites with the help of Ed Medina of the USGS. This characterization is preliminary and will be updated in the future. Information may also be available for some of the USNSN sites that were historically occupied by previous types of seismic system such as WWSSN, RSTN, or LRSM.

Table 9.1 USNSN Site Conditions

Site	Installation	Conditions
AAM	borehole	80m deep bedrock below glacial till
BINY	pad	bedrock - slate
BLA	borehole	bedrock
CBKS	pad	hard clay soil
CBM	pier	bedrock
CCM	pad	bedrock - within limestone cavern
CEH	vault-pier	soft sediments - old WWSSN site
EYMN	pad	bedrock
GOGA	pad	soft soil
GWDE	pad	soft soil
HKT	pad	within salt mine
HRV	vault-pier	bedrock - Oak Ridge Observatory.
JFWS	pad	bedrock - old zinc mine
LBNH	pad	granite outcrop
LSCT	pad	boulders
LTX	pads	shallow limestone bedrock
MCWV	adit-pad	unconsolidated bedrock
MIAR	pad	soft soil
MYNC	pad	soft soil
OXF	vault-pier	soft sediments - old WWSSN site
RSNY	borehole	bedrock - old RSTN site
RSSD	borehole	bedrock - old RSTN site
SSPA	borehole	100m deep in bedrock
WMOK	?	bedrock
YSNY	pad	soft soil

Table 9.2 Possible Future Sites

Site	Installation	Conditions
XXIN	pad	limestone cavern
XXMS	borehole	soft sediment
OSOH	pad	bedrock -Perkins Observatory

10.0 Network Simulation Internet WWW Home Pages

In order to distribute the results of network simulations in Sections 5 and 6 we have established a World Wide Web (WWW) Home Page on the Internet with the Universal Resource Locator, http://www.scubed.com/products/eus. Also, some files are available by anonymous file transfer protocol (FTP) at ftp.scubed.com (192.31.70.208) in the directory pub/eus.

11.0 Plans For Year 2

Plans for the second year of work include:

1) collection of additional noise models for all USNSN and cooperative stations,

2) collection of additional ground truth locations for validation of location uncertainty predicted by network simulations,

3) regionalization of the eastern US region for Pn, Pg, Sn, and Lg attenuation and velocity models, and

4) development of a simulation capability of focal mechanism and moment tensor estimation methods.

12.0 Acknowledgments

We would like to thank Ray Buland of the USGS/NEIC for providing useful detection and location information, John Claassen of SANDIA for an improved NetSim code and a revised noise database, Dean Clauter of AFTAC for providing additional noise data at selected sites, Tim Ahern of IRIS and Luciana Astiz of UCSD a copy of the IRIS noise database, Kevin Hutchenson, John Coyne, and Ron Cook of the Center for Monitoring Research for new noise data from the GSETT-3, Bob North of the Canadian Geological Survey for Canadian noise data, Martin Chapman of VPI for noise data and regional velocity models, and Ed Medina and Kent Anderson of the USGS Seismological Laboratory for information on USNSN site characteristics.

13.0 References

Barker, T. G., K. L. McLaughlin, and J. L. Stevens (1994), "Network Identification Capability Evaluation (NICE)," S-CUBED Technical Report SSS-TR-94-14701 submitted to ARPA, July.

Barker, T. G., W. L. Rodi, J. M. Savino (1986), "Modeling of Network Identification Capability," Final S-CUBED Report SSS-R-86-8033 submitted to DARPA.

Basham, P. W., and K. Whitham (1971), "Seismological Detection and Identification of Underground Nuclear Explosions," *Publications of the Earth Physics Branch Vol. 41, #9*, Department of Energy Mines and Resources, Ottawa Canada.

Bollinger. G. A., M. C. Chapman, and T. P. Moore (1980), "Central Virginia Regional Seismic Network: Crustal Velocity Structure in Central and Southwestern Virginia," NUREG/CR-1217, prepared for the U.S. Nuclear Regulatory Commission.

Booker, A. H. (1964), "Estimation of Network Capability," Prepared for Air Force Applications Center Wash. D.C., DATDC Report # 98.

Buland, R. (1993), "United States National Seismographic Network," U.S. Geological Survey Report prepared for the U.S. Nuclear Regulatory Commission, report NUREG/CR-6085.

Carts, D. A. and G. A. Bollinger (1981), "A Regional Crustal Velocity Model for the Southeastern United States," *Bull. Seism. Soc. Am., 71*, 1829-1847.

Chun, K. Y., G. F. West, R. J. Kokoski and C. Samson (1987), "A Novel Technique for Measuring Lg Attenuation - Results from Eastern Canada Between 1 to 10 Hz," *Bull. Seism. Soc. Am., 77*, 398-419.

Ciervo, A., S. Sanemitsu, D. Snead, R. Suey, and A. Watson (1985), "User's Manual for SNAP/D: Seismic Network Assessment Program for Detection," Pacific Sierra Research Corporation Report 1027B.

Ebel, J. E. (1994), "The m_bLg(f) Magnitude Scale: A Proposal for Its Use for Northeastern North America," *Seism. Res. Lett. 65*, 157-166.

Goncz, J. H., W. C. Dean, Z. A. Der, A. C. Lees, K. L. McLaughlin, T. W. McElfresh, and M. E. Marshall (1987), "Propagation and Excitation of Lg, Sn, and P-Pn Waves from Eastern United States Earthquakes by Regression Analysis of RSTN Data," TGAL-86-7, Teledyne Geotech, Alexandria, Virginia.

Gupta, I. N. and K. L. McLaughlin (1987), "Attenuation of Ground Motion in the Eastern United States," *Bull. Seism. Soc. Am., 77*, 366-383.

Gupta, I. N., K. L. McLaughlin, R. A. Wagner, R. S. Jih, and T. W. McElfresh (1989), "Seismic Wave Attenuation in Eastern North America," EPRI Report NP-6304.

Hasegawa, H. (1985), "Attenuation of Lg Waves in the Canadian Shield," *Bull. Seism. Soc. Am., 75,* 1569-1582.

Kelly, E. J., and R. T. Lacoss (1969), "Estimation of Seismicity and Network Detection Capability," MIT Lincoln Lab, Tech Note 41.

Luetgert, J. H., H. M. Benz, S. Madabhushi (1994), "Crustal Structure Beneath the Atlantic Coastal Plain of South Carolina," *Seism. Res. Lett. 65,* 180-191.

North, R. (1994), "The Canadian National Seismograph Network," *Annali di Geofisica XXXVII,* 1045-1048, 1994

North and Beverley (1994), "The Canadian National Seismograph Network," *IRIS Newsletter XIII No. 2,* Summer 1994

Nuttli, O. W. (1981), "Similarities and Differences Between Western and Eastern United States Earthquakes, and Their Consequences for Earthquake Engineering," in *Earthquakes and Earthquake Engineering: The Eastern United States,* J. E. Beavers, Editor, Ann Arbor Science Publishers, Ann Arbor, Michigan, 25-51.

Pechmann, J. C., W. R. Walter, Susan J. Nava, and W. J. Arabasz (1995), "The February 3, 1995 ML 5.1 Seismic Event in the Trona Mining District of Southwestern Wyoming," *SRL 66,* 25-34.

Sereno, T. J, S. R. Bratt, and G. Yee (1990), "NetSim: A Computer Program for Simulating Detection and Location Capability of Regional Seismic Networks," SAIC Report 90-1163 submitted to DARPA.

Singh, S., and R. B. Herrmann (1983), "Regionalization of Crustal Coda Q in the Continental United States," *J. Geophys. Res., 88,* 527-538.

Street, R. L. (1976), "Scaling Notheastern United States/Southeastern Canada Earthquakes by Their Lg Waves," *Bull. Seism. Soc. Am., 66,* 1525-1538.

Wirth, M. H. (1970), "Estimation of Network Detection and Location Capability," prepared for Air Force Technical Applications Center, Wash. D.C.

NRC FORM 335 (2-89) NRCM 1102, 3201, 3202

U.S. NUCLEAR REGULATORY COMMISSION

BIBLIOGRAPHIC DATA SHEET

(See instructions on the reverse)

1. REPORT NUMBER (Assigned by NRC, Add Vol., Supp., Rev., and Addendum Numbers, If any.)
NUREG/CR-6448, Vol. 1
SSS-TR-95-15216

2. TITLE AND SUBTITLE
Evaluation of National Seismograph Network Detection Capabilities

Annual Report, July 1994 - July 1995

3. DATE REPORT PUBLISHED
MONTH: March
YEAR: 1996

4. FIN OR GRANT NUMBER
L2170

5. AUTHOR(S)
K.L. McLaughlin and T.J. Bennett

6. TYPE OF REPORT
Annual

7. PERIOD COVERED (Inclusive Dates)
7/94 - 7/95

8. PERFORMING ORGANIZATION - NAME AND ADDRESS (If NRC, provide Division, Office or Region, U.S. Nuclear Regulatory Commission, and mailing address; if contractor, provide name and mailing address.)

S-CUBED Division of Maxwell Laboratories, Inc.
P.O. Box 1620
La Jolla, CA 92038

9. SPONSORING ORGANIZATION - NAME AND ADDRESS (If NRC, type "Same as above"; if contractor, provide NRC Division, Office or Region, U.S. Nuclear Regulatory Commission, and mailing address.)

Division of Engineering Technology
Office of Nuclear Regulatory Research
U.S. Nuclear Regulatory Commission
Washington, DC 20555-0001

10. SUPPLEMENTARY NOTES
E. Zurflueh, NRC Project Manager

11. ABSTRACT (200 words or less)

This first annual report presents detection thresholds, detection probabilities, and location error ellipse projections for the United States National Seismic Network (USNSN) with and without cooperative stations in the eastern United States. Network simulation methods are used with spectral noise levels at stations to simulate the processes of excitation, propagation, detection, and processing of seismic phases.

The USNSN alone should be capable of detecting 4 or more P waves for shallow crustal earthquakes in nearly all of the eastern and central United States at the magnitude 3.8 level. When cooperative stations are added, the network should be capable of detecting 4 or more P waves from events 0.2 to 0.3 magnitude units lower. The planned expansion of the USNSN and cooperative stations should improve detection levels by an additional 0.2 to 0.3 magnitudes units in many areas. Location uncertainties for the USNSN can be significantly improved by addition of real-time cooperative stations. Median error ellipses for magnitude 4.5 earthquakes depend strongly on location, but uncertainties should be less than 100 km^2 in the central United States and degrade to 200 km^2 or more off-shore and south and north of the international boundaries. Close cooperation with the Canadian National Network should substantially improve detection thresholds and location uncertainties along the Canadian border.

12. KEY WORDS/DESCRIPTORS (List words or phrases that will assist researchers in locating the report.)

Detection Threshold
Detection Probability
Location Error
Network Simulation

13. AVAILABILITY STATEMENT
Unlimited

14. SECURITY CLASSIFICATION
(This Page) Unclassified
(This Report) Unclassified

15. NUMBER OF PAGES

16. PRICE

NRC FORM 335 (2-89)

Federal Recycling Program

UNITED STATES
NUCLEAR REGULATORY COMMISSION
WASHINGTON, D.C. 20555-0001

OFFICIAL BUSINESS
PENALTY FOR PRIVATE USE, $300

FIRST CLASS MAIL
POSTAGE AND FEES PAID
USNRC
PERMIT NO. G-67

120555139531 1 1ANIRA
US NRC-OADM
DIV FOIA & PUBLICATIONS SVCS
TPS-PDR-NUREG
2WFN-6E7
WASHINGTON DC 20555